Localization and protein-protein interactions of protein kinase CK2 suggest a chaperone-like activity is integral to its function in *M. oryzae*

Lianhu Zhang[1*], Dongmei Zhang[1*], Yunyun Chen[1], Wenyu Ye[2], Qingyun Lin[2], Guodong Lu[1], Daniel J. Ebbole[1,3], Stefan Olsson[1,4,§] & Zonghua Wang[1,2,5§]

[1]State Key Laboratory for Ecological Pest Control of Fujian and Taiwan Crops, College of Plant Protection, Fujian Agriculture and Forestry University, Fuzhou 350002, China.
[2]College of Life Sciences, Fujian Agriculture and Forestry University, Fuzhou 350002, China.
[3]Department of Plant Pathology and Microbiology, Texas A&M University, College Station, Texas 77843, U.S.A.
[4]Plant Immunity Center, Haixia Institute of Science and Technology, Fujian Agriculture and Forestry University, Fuzhou 350002, China.
[5]Minjing University, Fuzhou 350018, China.

*These authors contributed equally to this work

§ These authors jointly supervised the work

Abstract

CK2 is known as a constitutively active, conserved serine/threonine kinase in eukaryotes and was investigated in the model fungus *Magnaporthe oryzae*. GFP fusions to CK2 subunits demonstrated nucleolar localization, although the catalytic subunit still localized to nucleoli in the absence of either regulatory subunit. In contrast, localization near septa, required all three subunits. Appressoria contain a filamentous form of CK2. The ~1300 proteins co-immunoprecipitating with the catalytic subunit were highly enriched for those known to reside at septa and nucleoli and of these, many were also found to be intrinsically unfolded proteins. Furthermore, a large proportion of these proteins contain a CK2 phosphorylation motif that has been proposed to function to destabilize and unfold alpha helixes. This

suggests a role for CK2 in the formation of protein aggregates through interaction with its substrates. Examining gene expression profiles, we find a correlation of CK2 expression with genes for protein disaggregation and autophagy. Our observations support the view that CK2 plays a general role in controlling formation of discrete regions (membraneless organelles), such as the nucleolus, through aggregation and disaggregation of many of its target proteins.

Introduction

Since its discovery (Meggio and Pinna, 2003), the constitutive serine/threonine (S/T) kinase activity of CK2 and the increasing number of proteins it has been shown to phosphorylate have puzzled scientists (Ahmad et al., 2008; Götz and Montenarh, 2016; Meggio and Pinna, 2003). Indeed CK2 has been implicated in a wide range of cellular processes (Götz and Montenarh, 2016). The typical CK2 holoenzyme is a heterotetrameric structure consisting of 2 catalytic α-units and 2 regulatory β-subunits (Ahmad et al., 2008). In mammals, there exist two different alpha subunits α (a1) and α' (a2) and the enzyme can contain any combination of α-subunits (α1α1, α1α2, α2α2) combined with the β-subunits. The CK2 of *Saccharomyces cerevisiae*, also contains two different alpha- and two different β-subunits (b1 and b2) and deletion of both catalytic subunits is lethal (Padmanabha et al., 1990). CK2 has been extensively studied in the budding yeast *S. cerevisiae* (Padmanabha et al., 1990), however, functions of CK2 involved in multicellularity might be obscured in yeast. In comparison to yeast, filamentous fungi have many different cell types that allow detailed exploration of cellular differentiation and multicellular development (Shlezinger et al., 2012) and this, in combination with haploid life-cycles, well characterized genomes, and efficient methods for targeted gene replacement, makes fungi like *M. oryzae* and *Fusarium graminearum* good model systems for molecular

studies of basic eukaryote functions including cell-cell communication (Cavinder et al., 2012; Ebbole, 2007). As plant pathogens, developmental processes needed for symbiosis can also be explored. We focused our study on *M. oryzae* one of the most important rice crop pathogens worldwide (Dean et al., 2012).

Our results show that *M. oryzae* CK2 holoenzyme (MoCK2) accumulates in the nucleolus, localizes in structures near septal pores, and assembles to form a large ring structure perpendicular to the appressorium penetration pore. The large-scale structures formed by CK2 protein kinase, combined with our finding of the interaction of CK2 with substrates associated with the location of CK2 enzyme aggregation, suggests that CK2 may control substrate stability and localization near their sites of action. Furthermore, CK2 interacts preferentially with proteins annotated as being intrinsically disordered carrying a phosphorylation motif that can destabilize alpha helix folding (Zetina, 2001). It has been shown for the specific case of CK2 in relation to the intrinsically highly disordered SRP40 protein (yeast), with Nopp140 and Nolc1 as common synonyms for homologues in other organisms, that SRP40 becomes phosphorylated to varying degrees by CK2 with effects on the SRP40 conformation, binding, and aggregation properties important for the diverse functions of the protein (Na et al., 2018; Tantos et al., 2013). Taken together, our work provides further evidence supporting the view (Zetina, 2001) that one of the main roles for the CK2 holoenzyme is as a general inducer of binding and conformational changes in intrinsically disordered proteins.

RESULTS

Deletion of MoCK2 components

We identified one CKa catalytic subunit ortholog (MoCka1, MGG_03696) and two MoCKb regulatory subunit orthologs (MoCKb1, MGG_00446 and MoCKb2, MGG_05651) (Figure 1 Supplement 1) based on BLASTp analysis using protein sequences for the CK2 subunits of *S. cerevisiae,* CKa1, CKa2, CKb1 and CKb2 (Padmanabha et al., 1990). Filamentous fungi have just one highly conserved catalytic subunit. In the case of *F. graminearum*, two genes with homology with CKa were identified previously (Wang et al., 2011), one that is highly conserved (we name FgCKa1), and one that is CKa-like (named FgCKa2). It remains to be determined if FgCKa2 is actually a CK2 subunit (Figure 1 Supplement 2-5). Targeted deletions of the two regulatory subunits succeeded (Figure 2a, b Figure 1 a, b and Table 1 for list of strains and their abbreviations). Attempts to delete the catalytic subunit, CKa, were unsuccessful, consistent with the essential role of CK2 activity (Hermosilla et al., 2005). The most obvious visible phenotype of the CKb mutants (strain b1 and b2) in culture was reduced growth rate (Figure 5 a, b and Figure 2 a, b) and conidial morphology in that they produced few conidia and those that were produced had fewer conidial compartments (Figure 2c).

Subcellular localization of CK2 subunits

To assess the localization of the three CK2 subunits, we constructed N-terminal GFP fusions of all three proteins (Filhol et al., 2003) GFP-MoCKa, GFP-MoCKb1 and GFP-MoCKb2 (strains GfpA, GfpB1 and GfpB2 respectively Table 1). All three strains showed the same growth rate, morphology (data not shown) and pathogenicity (Figure 3) as the control strain Ku80. The CKa and CKb1&2 fusion proteins localized to nuclei and prominently to nucleoli and, interestingly, to both sides of septal pores in hyphae (Figure 4 a-e) and conidia (Figure 4 Supplement 1). The RNA levels for the GFP fusion genes in these strains were elevated ~10 to 15-fold over the control level (Figure 5 Supplement 1 and Figure 4 Supplement 2).

We then tested if the localization to septa and nucleoli were dependent on the association with the other subunits of the holoenzyme. We had measured *MoCka* expression in the two *Mockb* mutants (b1 and b2) using qPCR and noted it was downregulated two- to three-fold compared to the background control strain Ku80 (Figure 5 a). We constructed strains that over-express GFP-CKa in deletion strains b1 and b2 (strains b1GfpA and b2GfpA). Expression of GFP-CKa was elevated 25-fold and 15-fold in the b1GfpA and b2GfpA strains, respectively (Figure 5b). Localization to GFP-MoCKa to septa was not observed (Figure 4 f, g), however, nucleolar localization of GFP-MoCKa was clear in the b1GfpA and b2GfpA strains. To test if over-expression of any one of the CKb proteins could rescue the effect of the deletion of the other CKb, we constructed GFP-CKb overexpression strains in both CKb mutants (strains b1GfpB2 and b2GfpB1 Table 1). As noted above, the overexpression of either of the two CKbs in the control strain Ku80 showed normal localization to septa and nucleolus (Figure 4 c, e, h, i) but the overexpression in the CKb deletion strains could not rescue normal localization (Figure 4 h,i). Furthermore, both GFP-MoCKb1 and GFP-MoCKb2 appeared to localize to nuclei but were excluded from nucleoli in the b2GfpB1 and b1GfpB2 strains, respectively. A limited restoration of conidial production and morphology defect of *ΔMockb1&2* deletions (strains b1 and b2) was observed in b1GfpA and b2GfpA (Figure 5 c, d, e). In addition, a significant restoration of growth rate was detected (Figure 6 a, b, d, e).

Infection phenotypes of CKb deletions

Deletion of CK2 genes has been shown to have effects on both growth and infection in *F. graminearum* (Wang et al., 2011) and we also found this to be the case for *M. oryzae* (Figure 6 c). Conidiation was virtually absent in both *ΔMockb1* and *ΔMockb2* deletion mutants (strains b1 and b2), thus, we used mycelial plugs to test for infection (Liu et al., 2010; Talbot et al., 1996). Compared to the background strain Ku80, mutants lacking one of the MoCK2b components had severely reduced or complete

lost pathogenicity on intact leaves. However, wound inoculated leaves were impacted by the mutants (Fig 6c). Overexpression of MoCka in the *ΔMockb1* and *ΔMockb2* lines (strains b1GfpA and b2GfpA) allowed sufficient conidia production to perform conidial inoculations. Small lesions were observed in both cases, indicating that Ckb subunits are not required for pathogenesis (Fig 6d).

Overexpression of the MoCkb1 subunit in strain b2, strain b2GfpB1, restored growth rate and improved conidiation (Figure 6 Supplement 1). In contrast, overexpression of MoCkb2 in strain b1, strain b1GfpB2 did not restore growth or conidiation. There was a limited but detectable restoration of pathogenicity in spore inoculation of strain b2GfpB1 compared to strain b2 and in mycelial inoculation of unwounded plants of strain b1GfpB2 compared to strain b1. This suggests that overexpression of MoCkb2 in the *ΔMockb1* mutant was unable to compensate for vegetative functions but could partially suppress the pathogenicity defect.

CKa localization in appressoria

Since we found large effects in infection of the deletion of the CKb components we decided to investigate localization of GFP-CKa in the appressoria. As in hyphae and conidia, GFP-CKa (strain GfpA) localizes to nuclei (Figure 7a top row and Figure 7 Supplement 1b), to the septa between the appressorium and the germ tube (Figure 7 Supplement 1) and also assembles a large ring structure perpendicular to the penetration pore (Figure 7 b-d, Figure 7 Supplement 1, Figure 7 Supplement 2 for ring size measurements, and movies associated with the images of Figure 7b-d showing 3D rotations to visualize the ring and the appressorium). MoCKa nuclear localization was present in appressoria formed by the two CK2b deletion mutants (strains b1GfpA and b2GfpA) (Figure 7a middle and bottom row), however ring structures were not observed. Concentration of GFP-MoCKa in nucleoli is clear in

conidia, however, we could not clearly observe preferential nucleolar localization in appressoria. As can be seen in Figure 7d, the CK2 large ring structure is positioned perpendicular to the penetration pore where the F-actin-septin ring has been shown to form around the pore opening (Dagdas et al., 2012) (Figure 7d and 8 schematic drawing).

Identification of potential septal and nucleolar substrates for MoCK2 by GFP-CKa pulldown

The localization pattern suggested that CK2 may have substrates associated with septa and nucleolar function. To explore this, we performed co-immunoprecipitation to identify proteins interacting with CK2 using GFP-CKa as a "bait", and in addition to the bait, identified 1505 proteins (Supplementary File 1). We also searched the *M. oryzae* proteome for proteins containing the CK2 phosphorylation helix unfolding motif identified by Zetina (Zetina, 2001) using the FIMO tool at the MEMEsuit website (http://meme-suite.org/) and found 1465 proteins (Supplementary File 2) with the motif, out of a total of 12827 proteins annotated for *M. oryzae.*

There is the risk of false positives in the pulldown. We estimated the number of false positives and removed 155 (~10%) of the lower abundance proteins to arrive at a list of 1350 CKa interacting proteins (see Methods). We found 275 of these proteins contain at least one unfolding motif for alpha helixes. Thus, there is an overrepresentation of the motif among the pulldown proteins (Supplementary File 2) (P-value for the null hypothesis of same frequency as in the whole proteome = 4 E-19, Fisher's Exact test) lending support for the proposed role for this motif as a target for CK2 phosphorylation and protein unfolding. As also expected, the pulldown caught both CKb proteins.

Since CK2 localizes to septa we looked for known septal proteins in the pulldown. All previously identified proteins by Dagas et al. (Dagdas et al., 2012) that are involved in appressorium pore development, were found in the pulldown as was a protein annotated as the main Woronin body protein, Hex1 (MGG_02696). Since the Woronin body in Ascomycetes is tethered to the septal rim by Lah protein (Han et al., 2014; Ng et al., 2009; Plamann, 2009) we searched for a homologue in *M. oryzae* and found a putative MoLah (MGG_01625) with a similar structure as in *Aspergillus oryzae* (Han et al., 2014) that is also present in the pulldown. In addition to the Lah, 18 other intrinsically disordered septal pore associated proteins (Spa) were described for *Neurospora crassa* (Lai et al., 2012). We identified putative orthologs for 15 of the 18 Spa proteins in *M. oryzae* (Supplementary File 3). Of these putative MoSpa proteins, six were present in the CKa pulldown, Spa3 (MGG_02701), Spa5 (MGG_13498), Spa7 (MGG_15285), Spa11 (MGG_16445), Spa14 (MGG_03714) and Spa 15 (MGG_15226). Spa3, Spa5 and Spa15 also contain the CK2 phosphorylation alpha helix unfolding motif (Supplementary File 1).

To further explore the hypothesis that CK2 could interact with and possibly phosphorylate intrinsically unfolded proteins we used the FuncatDB (http://mips.helmholtz-muenchen.de/funcatDB/) to make a functional classification of the pulldown proteins including those containing the alpha helix unfolding motif (Zetina, 2001). We found strong overrepresentation for proteins involved in rRNA processing among the pulldown proteins containing the alpha helix unfolding motif as well as for proteins that, themselves, are known to interact with other proteins, DNA, and RNA (Supplementary File 4). These classes of proteins are enriched for intrinsically disordered proteins. Such intrinsically disordered proteins can interact with each other to form ordered subregions that have been described as membraneless organelles, such as nucleoli (Wright and Dyson, 2015). Since CK2 localizes to the nucleolus we were especially interested in the interaction of CK2 with

nucleolar localized proteins. We identified homologues to the well described *S. cerevisiae* nucleolar proteins and found a total of 192 proteins in *M. oryzae* homologous to yeast nucleolar proteins (Supplementary File 5). We found 120 (63%) of the nucleolar proteins in the pulldown and 60 of these (50% of the ones found) had the alpha helix unfolding motif (Supplementary File 1 and 4). The nucleolar proteins were highly overrepresented in the pulldown (P-value for the null hypothesis of same frequency as in the whole proteome 9E-43 Fisher's Exact test) (Supplementary File 5) compared to the whole proteome as was also nucleolar proteins having the unfolding motif (P-value for the null hypothesis of same frequency as in the whole proteome 2E-13 Fisher's Exact test) (Supplementary File 5).

Ck2 is known to interact with the disordered nucleolar protein SRP40 that has a multitude of CK2 phosphorylation sites and in addition CK2 is known to change the protein binding activity towards other proteins depending the SRP40 phosphorylation status. When SRP40 becomes highly phosphorylated it binds to and inhibits CK2 activity in a negative feedback loop ensuring that CK2 phosphorylation level will balance (Tantos et al., 2013; Na et al., 2018). We identified a putative MoSRP40 (MGG_00613) and it is disordered in a similar way as other SRP40 proteins and it is well conserved in filamentous fungi (Supplementary File S8). The MoSRP40 protein was highly represented in the CKa pulldown indicating that it interacts with CKa (Supplementary File S1).

Interestingly, proteins that are imported into mitochondria and involved in oxidative phosphorylation ("02.11 electron transport and membrane-associated energy conservation" category from Funcat) (Supplementary File 4) were enriched in the pulldown proteins (60 of 130 in the whole proteome, P-value for the null hypothesis of same frequency as in the whole proteome 1.0E-29). In contrast with septal and nucleolar interacting proteins, the mitochondrial proteins were not enriched for the known unfolding motif.

There was no enrichment for specific pathogenicity related proteins (Funcat category 32.05 disease, virulence and defence) (Supplementary File 4). This is generally true within the whole Funcat category related to stress and defence (32 CELL RESCUE, DEFENSE AND VIRULENCE) with the exception of proteins involved in the unfolded protein response (32.01.07 unfolded protein response) (e.g. ER quality control), which were overrepresented. This is notable since an involvement of CK2 in protein import into the ER has be established (Wang and Johnsson, 2005). An association of pathogenicity related proteins with CK2 was not expected because of the *in vitro* growth conditions of the experiment.

Interestingly, five putative S/T phosphatases (MGG_03154, MGG_10195, MGG_00149, MGG_03838, MGG_06099) were in the pulldown set of proteins (Supplementary File 1). Conceivably these might de-phosphorylate CKa substrates as well as substrates of other kinases to expand the reach of CK2 in regulating the phosphoproteome. To examine the relationship between the expression of CK2 and these phosphatases, we downloaded expression data from a range of experiments with *M. oryzae* and plotted the expression of the five phosphatases found in the pulldown, and an S/T phosphatase not found in the pulldown, as a function of the CKa expression. We found that two of the S/T phosphatases present in the pulldown were strongly correlated with CKa expression and the others were less strongly correlated (Figure 9).

CKa expression correlates with expression of genes associated with disaggregation and autophagy

Since CK2 activity has the potential to favour protein-protein binding between intrinsically disordered proteins it consequently also has the potential to enhance protein aggregation. Some of these unfolded proteins may trigger the unfolded

protein response involved in disaggregation. Hsp104 is a disaggregase that cooperates with Yjdg1 and SSa1 to refold and reactivate previously denatured and aggregated proteins (Glover and Lindquist, 1998). Alternatively, accumulated aggregates may be degraded through autophagy since these kinds of aggregates are too big for proteasome degradation (Wong and Cuervo, 2010). If this is the case, CK2 upregulation should be accompanied by higher autophagy flux or at least there should not be low expression of key autophagy genes when CK2 expression is high (Wong and Cuervo, 2010). Atg8 is a key autophagy protein for which its turnover rate can reflect autophagy flux (Klionsky et al., 2016). To test this hypothesis, we used the expression data we downloaded for plant infection experiments with *M. oryzae* and also for another fungal plant pathogen, *F. graminearum*, that has rich transcriptomic data available (see methods), to examine expression of HSP104, YDJ1, SSA1, and ATG8 relative to CKa.

For *M. oryzae*, we found an approximately 60-fold increase in MoHSP104 expression associated with a doubling of MoCka transcript levels. With increasing expression of MoCka the MoHSP104 levels did not increase further. MoSSA1 expression had a similar pattern to MoHSP104 with a 16-fold increase across the initial 2-fold increase in MoCka expression. For MoYDJ1, expression increased with MoCKa expression, but not as dramatically (Fig 10). For *M. oryzae*, we find a log-log linear relationship between the MoCKa expression and MoAtg8 expression (Figure 10).

In the case of *F. graminearum*, we also found increased expression of all of the genes correlated with FgCKa expression across a large range of experiments (Figure 10 Supplement 1a). Within the *F. graminearum* experiments a time course experiment was selected to examine expression of these genes during the course of infection. Once again, the relationship could be observed (Figure 10 Supplement 1b), furthermore, FgCK2a expression increased during the course of infection (Figure 10 Supplement 2). Overall, these correlations support the hypothesis that protein

291 disaggregation and autophagy are increasingly needed to remove protein aggregates
292 stimulated to form by increasing levels of CKa and its activity in the cell.

293

294 **Discussion**

295 The analysis of the *MoCKb* mutants and the localization of the GFP-labelled MoCK2
296 proteins showed that all identified MoCK2 components are needed for normal
297 function and also normal localization. Localization to septa requires all three subunits,
298 presumably as the holoenzyme. Mutation of either CKb subunit blocks nucleolar
299 localization of the other CKb subunit. Surprisingly, nucleolar localization of CKa was
300 observed in the CKb mutants. This shows that the holoenzyme is not required for
301 CKa localization to the nucleolus. It seems likely that CKb1 and CKb2 must interact
302 with each other in order to interact with CKa, and that CKa is required for movement
303 of CKb subunits into the nucleolus as the holoenzyme.

304 The pattern of localization to septa (Figures 4) observed is remarkably similar to that
305 displayed by the Woronin body tethering protein AoLah from *A. oryzae* (Figure 4b in
306 (Han et al., 2014)). The pulldown experiments demonstrate that CK2 interacts with
307 proteins that function in septum formation and function, including the MoLah
308 ortholog, supporting the view that localization of the GFP-fusion proteins gives a
309 proper representation of CK2 localization. Our results thus demonstrate that the
310 MoCK2-holoenzyme assembles as a large complex near, and is perhaps tethered to,
311 septa, possibly through binding to MoLah. Since septal pores in fungi are gated (Shen
312 K-F. et al., 2014), as are gap junctions and plasmodesmata in animal and plant tissue,
313 respectively (Ariazi et al., 2017; Kragler, 2013; Neijssen et al., 2005), CK2 has a
314 potential to play a general role in this gating.

315

316 The crystal structure suggested that CK2 can form filaments and higher-order
317 interactions between CK2 holoenzyme tetramer units, and based on this it has been
318 predicted that autophosphorylation between the units could occur to down-regulate
319 activity (Litchfield, 2003; Poole et al., 2005). Filament formation has been shown to
320 occur *in vitro* (Glover, 1986; Seetoh et al., 2016; Valero et al., 1995) and *in vivo*
321 (Hübner et al., 2014). Several forms of higher order interactions have been predicted,
322 and it has been demonstrated that at least one of these has reduced kinase activity
323 (Poole et al., 2005; Valero et al., 1995). However, in our localization experiments
324 focused on septa, we cannot distinguish if the large structure is due to co-localization
325 of the CK2 with another protein, such as the MoLah ortholog, or if CK2 is in an
326 aggregated form near septa. Since MoLah has the characteristics of an intrinsically
327 disordered protein (Han et al., 2014), and CK2 has been proposed to interact with
328 proteins to promote their disordered state (Zetina, 2001; Tantos et al., 2013; Na et al.,
329 2018), we favour the view that CK2 interacts with MoLah and other proteins to form
330 a complex near septa.

331 The large ring observed in appressoria may be a true filament of CK2 in a relatively
332 inactive state that is a store for CK2 so that upon infection, it can facilitate rapid
333 ribosome biogenesis, appressorial pore function, and other pathogenesis-specific
334 functions.

335 Our pulldown experiment with GFP-CKa further showed that there was a strong
336 overrepresentation of proteins interacting with CKa that contain known
337 phosphorylation motifs for unfolding of alpha-helixes and this is what would be
338 expected for intrinsically disordered proteins (Uversky, 2015; Zetina, 2001). The
339 finding of overrepresentation of this signal in the set of CK2 interacting proteins
340 corroborates the previous suggestion that CK2 is involved in the
341 destabilization/binding of intrinsically disordered proteins (Zetina, 2001; Tantos et al.,
342 2013; Na et al., 2018) and is consistent with the strong accumulation of both CK2 and

intrinsically disordered proteins in the nucleolus (Fig. 4a and b) (Frege and Uversky, 2015) and also at pores between cell compartments (Lai et al., 2012) (Figure 4d). In addition, and further supporting this conclusion, the six septal pore associated proteins (SPA) that we find in the CKa pulldown are homologues for intrinsically disordered proteins that are expected to form temporary gels that are used to reversibly plug septal pores and regulate traffic through septa (Lai et al., 2012). CK2 could actively be involved in the gelling/un-gelling of the regions near septa to create a membraneless organelle controlling the flow through septa. As a counterpart to CK2 in gelling/un-gelling, disaggregase activity involving the MoHSP104 complex, may be critical for control of this. The observation of transcriptional co-regulation between CKa and HSP104 supports this notion.

Previous studies of subcytosolic localization reveals that this enzyme is also associated with import into organelles. CK2 promotes protein import into endoplasmic reticulum (Wang & Johnsson, 2005) and into mitochondria during mitochondrial biogenesis and maintenance (Rao et al., 2011). CK2 phosphorylation has been shown to activate Tom22 precursors to assemble a functional mitochondrial import machinery (Rao et al., 2011). Although CK2 has been implicated to be located in mitochondria in earlier studies in other organisms, no proteomic study of yeast mitochondria has detected the presence of CK2 (Rao et al., 2011). Hence, we do not expect MoCK2 to be present in mitochondria, and we saw no evidence for mitochondrial localization. Of special interest was however the strong overrepresentation of mitochondrial proteins among the CKa pulldown proteins without the alpha helix phosphorylation unfolding motif (Supplementary File 4). Since these proteins need to be imported into mitochondria in an unfolded state, this may point to the existence of CKa phosphorylation and unfolding motifs other than the one identified by Zetina (Zetina, 2001) that help keep these proteins unfolded until they reach their destination inside the mitochondria.

To have such dynamic function as an unfolder of proteins by phosphorylation, CK2 should be partnered with phosphatases as counterparts and their activity may track CK2 activity. Consistent with this possibility, we found that two of the five S/T phosphatases that are present in the pulldown are strongly co-regulated with CKa (Figure 9), further supporting the view that CKa-dependent phosphorylation/dephosphorylation plays a major role in shaping protein interactions. Together with the high expression of CK2 in cells, this suggests an important function of CK2 as a general temporary unfolder of intrinsically disordered proteins, that comprise roughly 30 % of eukaryotic proteins (Vucetic et al., 2003), in a similar way as it is known to interact with SRP40 and influence its activity (Tantos et al., 2013; Na et al., 2018).

As MoCK2 is present in the cytoplasm and nucleoplasm it would generally assist intrinsically disordered proteins in protein interactions (Uversky, 2015). It also seems to be essential for assembling ribosomes containing large numbers of intrinsically disordered proteins (Uversky, 2015). All these functions also explains why CK2 is needed constitutively (Meggio and Pinna, 2003).

In the absence of well-functioning autophagy removing incorrectly formed larger protein aggregates, like those formed in brain cells of Alzheimer's patients (Zare-shahabadi et al., 2015), CK2 activity facilitates protein aggregate formation and hastens the progression of Alzheimer's disease (Rosenberger et al., 2016). Using publicly available transcriptome datasets we could show that CKa expression in *M. oryzae* and *F. graminearum* is strongly correlated to disaggregase and Atg8 expression (Figure 10), and thus autophagy, giving further support for a relationship of CK2 in facilitating the formation of protein aggregates from intrinsically unfolded proteins that are then subjected to autophagy. As autophagy is important to appressorium development (Liu and Lin, 2008; Kershaw and Talbot, 2009), it will be

of interest to further examine the role of the CK2 ring structure during appressorial development and infection.

Conclusion

We conclude that CK2 likely has an important general role in the correct assembly/disassembly of intrinsically disordered proteins as well as allowing these proteins to pass through narrow pores between cell compartments, in addition to its already suggested role in organelle biogenesis (Rao et al., 2011). Our results further point to one of the main functions of the CK2 holoenzyme as a general facilitator of protein-protein interactions important for a large range of cellular processes including a potential role for gel formation that creates membraneless organelles at septa through its likely interaction with, and modification of, intrinsically disordered proteins. We thus feel it appropriate to cite "Using basket terminology, one would say that CK2 looks like a "playmaker" not a "pivot": hardly ever does it make scores; nevertheless, it is essential to the team game" (Meggio and Pinna, 2003).

Methods

Fungal strains, culture, and transformation

The *M. oryzae* Ku80 mutant (constructed from the wild type Guy11 strain was used as background strain since it lacks non-homologous end joining which facilitates gene targeting (Villalba et al., 2008). Ku80 and its derivative strains (Table 1) were all stored on dry sterile filter paper and cultured on complete medium (CM: 0.6% yeast extract, 0.6% casein hydrolysate, 1% sucrose, 1.5% agar) or starch yeast medium (SYM: 0.2% yeast extract, 1% starch, 0.3% sucrose, 1.5% agar) at 25°C. For conidia production, cultures were grown on rice bran medium (1.5% rice bran, 1.5% agar) with constant light at 25°C. Needed genome and proteome FASTA files was

421 downloaded from an FTP-server at the Broad Institute
422 (ftp://ftp.broadinstitute.org/pub/annotation/fungi/magnaporthe/genomes/magnaporthe
423 _oryzae_70-15_8/). Fungal transformants were selected for the appropriate markers
424 inserted by the plasmid vectors. The selective medium contained either 600 μg/ml of
425 hygromycin B or 600 μg/ml of G418 or 50 μg/ml chlorimuron ethyl.

426

427 **MoCKb gene replacement and complementation**

428 Gene replacement mutants of *MoCKb1* encoding protein MoCKb1 were generated by
429 homologous recombination. Briefly, a fragment about 0.9 Kb just upstream of
430 *Mockb1* ORF was amplified with the primers 446AF and 446AR (Table 2), so was
431 the 0.7Kb fragment just downstream of *Mockb1* ORF amplified with the primers
432 446BF and 446BR (Table 2). Both fragments were linked with the hygromycin
433 phosphotransferase (*hph*) gene amplified from pCX62 (containing the fragment of
434 TrpC promoter and hygromycin phosphotransferase (*hph*) gene, HPH resistance).
435 Then the fusion fragments were transformed into protoplasts of the background strain
436 Ku80. The positive transformant *ΔMockb1* (strain b1, Table 1) was picked from a
437 selective agar medium supplemented with 600 μg/ml of hygromycin B and verified
438 by Southern blot.

439 For complementation of the mutant, fragments of the native promoter and gene
440 coding region were amplified using the primers 446comF and 446comR listed in
441 Table 2. This fragment was inserted into the pCB1532 to construct the
442 complementation vector using the XbaI and KpnI. Then this vector was transformed
443 into the protoplasts of strain b1. The positive complementation transformant, strain
444 b1B1, was picked up from the selective agar medium supplemented with 50μg/ml
445 chlorimuron ethyl.

As for the *ΔMoCKb1* deletion mutant, we constructed a knockout vector to delete the *MoCKb2* from the background strain Ku80. All the primers are listed in the Table 2. The 1.0Kb fragment upstream of *MoCKb2* ORF was amplified with the primers 5651AF and 5651AR, inserted into the plasmid pCX62 using the KpnI and EcoRI to get the pCX-5A vector. The 1.0Kb fragment downstream of *Mockb2* ORF was amplified with the primers 5651BR and 5651BR, inserted into the vector pCX-5A using BamHI and XbaI to construct the knockout vector pCX-5D. Then this vector was transformed into the protoplasts of Ku80. The positive transformants were picked up from the selective medium supplemented with the 600 μg/ml hygromycin B. For complementation of the resulting mutant, strain b2 (Table 1), fragments of the native promoter and gene coding region were amplified using the primers 5651comF and 5651comR listed in the Table 2. This fragment was inserted into pCB1532 to construct the complementation vector using the XbaI and XmaI. Then this vector was transformed into protoplasts of the strain b2. The positive complementation transformant, strain b2B2, was picked up from the selective agar medium supplemented with 50 μg/ml chlorimuron ethyl.

The construction of localization vectors

In order to detect the localization of MoCK2, we constructed localization vectors. The vector pCB-3696OE containing the RP27 strong promoter was used to detect the localization of GFP-MoCKa (strain GfpA). The vector pCB-446OE expressed under RP27 strong promoter was used to detect the localization of GFP-MoCKb1 (strain GfpB1). The vector pCB-5651OE expressed by RP27 strong promoter was used to detect the localization of GFP-MoCKb2 (strain GfpB2).

Analysis of conidial morphology, conidial germination and appressoria formation

Conidia were prepared from cultures grown on 4% rice bran medium. Rice bran medium was prepared by boiling 40g rice bran (can be bought for example through

Alibaba.com) in 1L DD-water for 30 minutes. After cooling pH was adjusted from to 6.5 using NaOH and 20 g agar (MDL No MFCD00081288) was added before sterilization by autoclaving (121ºC for 20 minutes). Conidia morphology was observed using confocal microscopy (Nikon $A1^{+}$). The Conidial germination and appressoria formation were incubated on hydrophobic microscope cover glass (Beckerman and Ebbole, 1996) (Fisherbrand) under 25℃ in the dark. Conidial germination and appressoria formation were examined at 24 h post-incubation (Beckerman and Ebbole, 1996; Ding et al., 2010).

Pathogenicity assay

Plant infection assays were performed on rice leaves. The rice cultivar used for infection assays was CO39. In short, mycelial plugs were put on detached intact leaves or leaves wounded by a syringe stabbing. These leaves were incubated in the dark for 24h and transferred into constant light and incubated for 5 days to assess pathogenicity (Talbot et al., 1996). For infections using conidial suspensions (1×10^5 conidia/ml in sterile water with 0.02% Tween 20) were sprayed on the rice leaves of 2-week-old seedlings.

RNA extraction and real-time PCR analysis

RNA was extracted with the RNAiso Plus kit (TaKaRa). First strand cDNA was synthesized with the PrimeScript RT reagent Kit with gDNA Eraser (TaKaRa). For quantitative real-time PCR, *MoCKa, MoCKb1*, and *MoCKb2* were amplified with the primers listed in Table 2. β-tubulin (XP_368640) was amplified as an endogenous control. Real-time PCR was performed with the TaKaRa SYBR Premix Ex Taq (Perfect Real Time) (Takara). The relative expression levels were calculated using the $2^{-\Delta\Delta Ct}$ method (Livak and Schmittgen, 2001).

Pulldown and identification of CKa interacting proteins

Total protein samples were extracted from vegetative mycelia of strain GFP-MoCKa and incubated with anti-GFP beads (Chromotek, Hauppauge, NY, USA) 90 minutes at 4°C with gentle shaking. After a series of washing steps, proteins bound to anti-GFP beads were eluted following the manufacturer's instruction. The eluted proteins were sent to BGI Tech (Shenzhen, Guangdong province, China) and analysed by mass spectrometry for analysis of sequence hits against the *M. oryzae* proteome. The transformant expressing GFP protein only was used as the negative control and the Ku80 was used as Blank control. Data from three biological replicates were analyzed against the background of proteins that were bound non-specifically to the anti-GFP beads in GFP transformant and in Ku80 to get the final gene list of genes that was pulldown with CKa (Supplementary File1).

Estimation of non-specific binding of proteins in the pulldown

We developed two methods to estimate the number of non-specific binding proteins found in the CKa pulldown. The first approach is a chemistry-based reasoning and assumes that the degree of unspecific association to the protein per protein surface area is the same for GFP specific hits and for the CK2 holoenzyme pulled down. Using this technique, we estimate that 44-132 proteins are false positive in the CKa pulldown (all proteins pulled down by GFP-Beads or the Beads already removed from the list) (Supplementary File 1). The Second approach is statistical where we assume that binding of the true interacting proteins to CKa are log-normally distributed related to the abundance of each protein in the pulldown, since the median is low and close to zero and negative amounts are impossible. Using the deviation from the theoretical distribution, with higher than expected amounts of a specific protein, for the less abundant proteins we estimate that 46-81 proteins found in the CKa pulldown (with controls subtracted) were false positive. The higher number was used to set a conservative threshold for which proteins should be included in the analysis (See Supplementary File 1 for details of both methods).

Finding *M. oryzae* proteins containing the helix unfolding motif

The MEME motif LSDDDXE/SLEEEXD (Zetina, 2001) was used to search through the proteome of *M. oryzae* using the FIMO tool at the MEMEsuite website (http://meme-suite.org/). Results were then downloaded and handled in MS Excel to produce a list of proteins with at least one motif hit (Supplementary File 2)

Analysis of CKa expression in relation to disaggregase related protein, Atg8 and Ser/Thr phosphatase expression

For *M. oryzae,* transcriptome experiment data was downloaded as sra/fastq files from Gene Expression Omnibus, https://www.ncbi.nlm.nih.gov/geo/and mapped onto the genome found at http://fungi.ensembl.org/Magnaporthe_oryzae/Info/Index. The procedure was the following: Gene Expression Omnibus (Barrett et al., 2012) was queried for SRA files originating from *M. oryzae* and the files downloaded. The conversion from SRA to Fastq was done using the SRA toolkit (http://ncbi.github.io/sra-tools). The resulting samples were subjected to quality control using FASTQC (Andrews, 2010). Quantification of RNA was performed using Kallisto with default settings (Bray 2016), the data was then normalized using the VST algorithm implemented in DESeq2 (Love et al., 2014).

For *F. graminearum* transcriptomic data (FusariumPLEX) was directly downloaded for mainly *in planta* experiments from the PlexDB database (http://www.plexdb.org/modules/PD_general/download.php?species=Fusarium). For each fungus an expression matrix with the different experiments as columns and gene id using the FGSG codes according to BROAD (ftp.broadinstitute.org/distribution/annotation/fungi/fusarium/genomes/fusarium_graminearum_ph-1) as rows were prepared. From the resulting matrixes (Supplementary Files 6 and 7) we used the data needed to plot expression of Atg8 vs CKa for the two fungi. In *M. oryzae* data are expressed as log2 of RPKM values. Similarly, for *F.*

graminearum, data were log2 of reported relative expression. Gene expression data used were from MoCKa, MoHSP104, FgHSP109, MoYDJ1, FgYDJ1, MoSSA1and Fg SSA1 homologues identified in this study as well as from MoAtg8 (MGG_01062) (Veneault-Fourrey, 2006), FgCKa (FGSG_00677) (Wang et al., 2011) and FgAtg8 (FGSG_10740) (Josefsen et al., 2012). Data from the *M. oryzae* expression matrix was also used for plotting MoCKa expression versus the expression of annotated serine/threonine phosphatases found in the CKa pulldown.

Data availability

The data that support the findings of this study are available from the corresponding authors upon request.

References

Ahmad, K.A., Wang, G., Unger, G., Slaton, J., and Ahmed, K. (2008). Protein kinase CK2 – A key suppressor of apoptosis. Adv. Enzyme Regul. *48*, 179–187.

Andrews, S. (2010). FastQC: a quality control tool for high throughput sequence data. Available online at Http://www.bioinformatics.babraham.ac.uk/projects/fastqc.

Ariazi, J., Benowitz, A., De Biasi, V., Den Boer, M.L., Cherqui, S., Cui, H., Douillet, N., Eugenin, E.A., Favre, D., Goodman, S., et al. (2017). Tunneling Nanotubes and Gap Junctions–Their Role in Long-Range Intercellular Communication during Development, Health, and Disease Conditions. Front. Mol. Neurosci. *10*.

Barrett, T., Wilhite, S.E., Ledoux, P., Evangelista, C., Kim, I.F., Tomashevsky, M., Marshall, K.A., Phillippy, K.H., Sherman, P.M., Holko, M., et al. (2012). NCBI GEO: archive for functional genomics data sets—update. Nucleic Acids Res. *41*, D991–D995.

Beckerman, J.L., and Ebbole, D.J. (1996). MPG1, a Gene Encoding a Fungal Hydrophobin of Magnaporthe grisea, Is Involved in Surface Recognition. MPMI *9*, 450–456.

Cavinder, B., Sikhakolli, U., Fellows, K.M., and Trail, F. (2012). Sexual Development and Ascospore Discharge in Fusarium graminearum. J. Vis. Exp.

578 Dagdas, Y.F., Yoshino, K., Dagdas, G., Ryder, L.S., Bielska, E., Steinberg, G., and Talbot, N.J. (2012). Septin-
579 mediated plant cell invasion by the rice blast fungus, Magnaporthe oryzae. Science *336*, 1590–1594.

580 Dean, R., Van Kan, J.A.L., Pretorius, Z.A., Hammond-Kosack, K.E., Di Pietro, A., Spanu, P.D., Rudd, J.J.,
581 Dickman, M., Kahmann, R., Ellis, J., et al. (2012). The Top 10 fungal pathogens in molecular plant pathology:
582 Top 10 fungal pathogens. Mol. Plant Pathol. *13*, 414–430.

583 Ding, S.-L., Liu, W., Iliuk, A., Ribot, C., Vallet, J., Tao, A., Wang, Y., Lebrun, M.-H., and Xu, J.-R. (2010). The
584 Tig1 Histone Deacetylase Complex Regulates Infectious Growth in the Rice Blast Fungus Magnaporthe
585 oryzae. PLANT CELL ONLINE *22*, 2495–2508.

586 Ebbole, D.J. (2007). Magnaporthe as a Model for Understanding Host-Pathogen Interactions. Annu. Rev.
587 Phytopathol. *45*, 437–456.

588 Filhol, O., Nueda, A., Martel, V., Gerber-Scokaert, D., Benitez, M.J., Souchier, C., Saoudi, Y., and Cochet, C.
589 (2003). Live-Cell Fluorescence Imaging Reveals the Dynamics of Protein Kinase CK2 Individual Subunits. Mol.
590 Cell. Biol. *23*, 975–987.

591 Frege, T., and Uversky, V.N. (2015). Intrinsically disordered proteins in the nucleus of human cells. Biochem.
592 Biophys. Rep. *1*, 33–51.

593 Glover, C.V. (1986). A Filamentous Form of Drosophila Casein Kinase II. J. Biol. Chem. *261*, 14349–14354.

594 Glover, J.R., and Lindquist, S. (1998). Hsp104, Hsp70, and Hsp40: A Novel Chaperone System that Rescues
595 Previously Aggregated Proteins. Cell *94*, 73–82.

596 Götz, C., and Montenarh, M. (2016). Protein kinase CK2 in development and differentiation (Review).
597 Biomed. Rep.

598 Han, P., Jin, F.J., Maruyama, J., and Kitamoto, K. (2014). A Large Nonconserved Region of the Tethering
599 Protein Leashin Is Involved in Regulating the Position, Movement, and Function of Woronin Bodies in
600 Aspergillus oryzae. Eukaryot. Cell *13*, 866–877.

601 Hermosilla, G.H., Tapia, J.C., and Allende, J.E. (2005). Minimal CK2 activity required for yeast growth. Mol.
602 Cell. Biochem. *274*, 39–46.

603 Hübner, G.M., Larsen, J.N., Guerra, B., Niefind, K., Vrecl, M., and Issinger, O.-G. (2014). Evidence for
604 aggregation of protein kinase CK2 in the cell: a novel strategy for studying CK2 holoenzyme interaction by
605 BRET2. Mol. Cell. Biochem. *397*, 285–293.

606 Josefsen, L., Droce, A., Sondergaard, T.E., Sørensen, J.L., Bormann, J., Schäfer, W., Giese, H., and Olsson, S.
607 (2012). Autophagy provides nutrients for nonassimilating fungal structures and is necessary for plant
608 colonization but not for infection in the necrotrophic plant pathogen Fusarium graminearum. *8*, 13.

609 Kershaw, M.J., and Talbot, N.J. (2009). Genome-wide functional analysis reveals that infection-associated
610 fungal autophagy is necessary for rice blast disease. Proc. Natl. Acad. Sci. *106*, 15967–15972.

611 Klionsky, D.J., Abdelmohsen, K., Abe, A., Abedin, M.J., Abeliovich, H., Acevedo Arozena, A., Adachi, H.,
612 Adams, C.M., Adams, P.D., Adeli, K., et al. (2016). Guidelines for the use and interpretation of assays for
613 monitoring autophagy (3rd edition). Autophagy *12*, 1–222.

614 Kragler, F. (2013). Plasmodesmata: intercellular tunnels facilitating transport of macromolecules in plants.
615 Cell Tissue Res. *352*, 49–58.

616 Lai, J., Koh, C.H., Tjota, M., Pieuchot, L., Raman, V., Chandrababu, K.B., Yang, D., Wong, L., and Jedd, G.
617 (2012). Intrinsically disordered proteins aggregate at fungal cell-to-cell channels and regulate intercellular
618 connectivity. Proc. Natl. Acad. Sci. *109*, 15781–15786.

619 Litchfield, D.W. (2003). Protein kinase CK2: structure, regulation and role in cellular decisions of life and
620 death. Biochem. J. *369*, 1–15.

621 Liu, X., and Lin, F. (2008). Investigation of the biological roles of autophagy in appressorium morphogenesis
622 in Magnaporthe oryzae. J. Zhejiang Univ. Sci. B *9*, 793–796.

623 Liu, W., Xie, S., Zhao, X., Chen, X., Zheng, W., Lu, G., Xu, J.-R., and Wang, Z. (2010). A homeobox gene is
624 essential for conidiogenesis of the rice blast fungus Magnaporthe oryzae. Mol. Plant. Microbe Interact. *23*,
625 366–375.

626 Livak, K.J., and Schmittgen, T.D. (2001). Analysis of Relative Gene Expression Data Using Real-Time
627 Quantitative PCR and the 2−ΔΔCT Method. Methods *25*, 402–408.

628 Love, M.I., Huber, W., and Anders, S. (2014). Moderated estimation of fold change and dispersion for RNA-
629 seq data with DESeq2. Genome Biol. *15*.

630 Meggio, F., and Pinna, L.A. (2003). One thousand-and one substrates of protein kinase CK2. FASEB J. *17*,
631 349–368.

632 Mehra, A., Shi, M., Baker, C.L., Colot, H.V., Loros, J.J., and Dunlap, J.C. (2009). A Role for Casein Kinase 2 in
633 the Mechanism Underlying Circadian Temperature Compensation. Cell *137*, 749–760.

634 Na, J.-H., Lee, W.-K., and Yu, Y. (2018). How Do We Study the Dynamic Structure of Unstructured Proteins:
635 A Case Study on Nopp140 as an Example of a Large, Intrinsically Disordered Protein. Int. J. Mol. Sci. *19*, 381.

636 Neijssen, J., Herberts, C., Drijfhout, J.W., Reits, E., Janssen, L., and Neefjes, J. (2005). Cross-presentation by
637 intercellular peptide transfer through gap junctions. Nature *434*, 83–88.

638 Ng, S.K., Liu, F., Lai, J., Low, W., and Jedd, G. (2009). A Tether for Woronin Body Inheritance Is Associated
639 with Evolutionary Variation in Organelle Positioning. PLoS Genet. *5*, e1000521.

640 Padmanabha, R., Chen-Wu, J.L.-P., Arnot, D.E., and Glover, C.V.C. (1990). Isolation, sequencing, and
641 disruption of the yeast CKA2 gene casein kinase II is essential for viability in Saccharomyces cerevisiae. Mol.
642 Cell. Biol. *10*, 4089–4099.

643 Plamann, M. (2009). Cytoplasmic Streaming in Neurospora: Disperse the Plug To Increase the Flow? PLoS
644 Genet. *5*, e1000526.

645 Poole, A., Poore, T., Bandhakavi, S., McCann, R.O., Hanna, D.E., and Glover, C.V. (2005). A global view of
646 CK2 function and regulation. Mol. Cell. Biochem. *274*, 163–170.

647 Rao, S., Gerbeth, C., Harbauer, A., Mikropoulou, D., Meisinger, C., and Schmidt, O. (2011). Signaling at the
648 gate: Phosphorylation of the mitochondrial protein import machinery. Cell Cycle *10*, 2083–2090.

649 Rosenberger, A.F.N., Morrema, T.H.J., Gerritsen, W.H., van Haastert, E.S., Snkhchyan, H., Hilhorst, R.,
650 Rozemuller, A.J.M., Scheltens, P., van der Vies, S.M., and Hoozemans, J.J.M. (2016). Increased occurrence of
651 protein kinase CK2 in astrocytes in Alzheimer's disease pathology. J. Neuroinflammation *13*.

652 Seetoh, W.-G., Chan, D.S.-H., Matak-Vinković, D., and Abell, C. (2016). Mass Spectrometry Reveals Protein
653 Kinase CK2 High-Order Oligomerization *via* the Circular and Linear Assembly. ACS Chem. Biol. *11*, 1511–
654 1517.

655 Shen K-F., Osmani A. S., Govindaraghavan M., and Osmani S. A. (2014). Mitotic rregulation of fungal cell-to-
656 cell connectivity through septal pores involves the NIMA kinase. Mol. Biol. Cell *25*, 763–775.

657 Shlezinger, N., Goldfinger, N., and Sharon, A. (2012). Apoptotic-like programed cell death in fungi: the
658 benefits in filamentous species. Front. Oncol. *2*.

659 Talbot, N.J., Kershaw, M.J., Wakley, G.E., De Vries, O.M., Wessels, J.G., and Hamer, J.E. (1996). MPG1
660 encodes a fungal hydrophobin involved in surface interactions during infection-related development of
661 Magnaporthe grisea. Plant Cell Online *8*, 985–999.

662 Tantos, A., Szrnka, K., Szabo, B., Bokor, M., Kamasa, P., Matus, P., Bekesi, A., Tompa, K., Han, K.-H., and
663 Tompa, P. (2013). Structural disorder and local order of hNopp140. Biochim. Biophys. Acta BBA - Proteins
664 Proteomics *1834*, 342–350.

665 Uversky, V.N. (2015). The multifaceted roles of intrinsic disorder in protein complexes. FEBS Lett. *589*,
666 2498–2506.

667 Valero, E., De Bonis, S., Filhol, O., Wade, R.H., Langowski, J., Chambaz, E.M., and Cochet, C. (1995).
668 Quaternary Structure of Casein Kinase 2 - Characterization of Multiple Oligomeric States and Relation with
669 its Catalytic Activity. J. Biol. Chem. *270*, 8345–8352.

670 Veneault-Fourrey, C. (2006). Autophagic Fungal Cell Death Is Necessary for Infection by the Rice Blast
671 Fungus. Science *312*, 580–583.

672 Villalba, F., Collemare, J., Landraud, P., Lambou, K., Brozek, V., Cirer, B., Morin, D., Bruel, C., Beffa, R., and
673 Lebrun, M.-H. (2008). Improved gene targeting in Magnaporthe grisea by inactivation of MgKU80 required
674 for non-homologous end joining. Fungal Genet. Biol. *45*, 68–75.

675 Vucetic, S., Brown, C.J., Dunker, A.K., and Obradovic, Z. (2003). Flavors of protein disorder. Proteins Struct.
676 Funct. Bioinforma. *52*, 573–584.

677 Wang, X., and Johnsson, N. (2005). Protein kinase CK2 phosphorylates Sec63p to stimulate the assembly of
678 the endoplasmic reticulum protein translocation apparatus. J. Cell Sci. *118*, 723–732.

679 Wang, C., Zhang, S., Hou, R., Zhao, Z., Zheng, Q., Xu, Q., Zheng, D., Wang, G., Liu, H., Gao, X., et al. (2011).
680 Functional Analysis of the Kinome of the Wheat Scab Fungus Fusarium graminearum. PLoS Pathog. *7*,
681 e1002460.

682 Wong, E., and Cuervo, A.M. (2010). Integration of Clearance Mechanisms: The Proteasome and Autophagy.
683 Cold Spring Harb. Perspect. Biol. *2*, a006734–a006734.

684 Wright, P.E., and Dyson, H.J. (2015). Intrinsically disordered proteins in cellular signalling and regulation.
685 Nat. Rev. Mol. Cell Biol. *16*, 18–29.

686 Zare-shahabadi, A., Masliah, E., Johnson, G.V.W., and Rezaei, N. (2015). Autophagy in Alzheimer's disease.
687 Rev. Neurosci. *26*.

688 Zetina, C.R. (2001). A Conserved Helix-Unfolding Motif in the Naturally Unfolded Proteins. Proteins Struct.
689 Funct. Genet. *44*, 479–483.

690

691 **Acknowledgements** We thank Dr. Guanghui Wang, Dr. Wenhui Zheng, Dr. Ya Li and
692 Dr. Huawei Zheng (Fujian Agriculture and Forestry University, Fuzhou, China) for
693 their helpful discussions. We thank Professor Jin-Rong Xu, Department of Botany
694 and Plant Pathology Purdue University, U.S.A. for providing the Ku80 strain. We
695 thank Dr. Bjoern Oest Hansen, Goettingen for help with mapping and constructing
696 the used *M. oryzae* transcriptome datafile from downloaded data. This work was
697 supported by the National Natural Science Foundation of China (U1305211),
698 National Key Research and Development Program of China (2016YFD0300700) and
699 National Natural Science Foundation for Young Scientists of China (Grant
700 No.31500118 and No.31301630), the 100 Talent Program of Fujian Province, and
701 USDA NIFA Hatch project 1013944.

702 **Authors' contributions** Conceived and designed the experiments: G. L., S. O. and Z.
703 W. Performed the experiments: L. Z., D. Z., Y. C., W. Y. and Q. L. Analysed the data:
704 L. Z., D. Z., D. J. E., S. O. and Z. W. Wrote the paper: L. Z., D. Z., D. J. E., S. O. and
705 Z. W.

706 **Competing interests statement** The authors declare that they have no competing
707 financial interests.

708 **Correspondence** and request for materials should be addressed to S.O.
709 (stefan@olssonstefan.com) or Z.W. (wangzh@fafu.edu.cn).

710

711

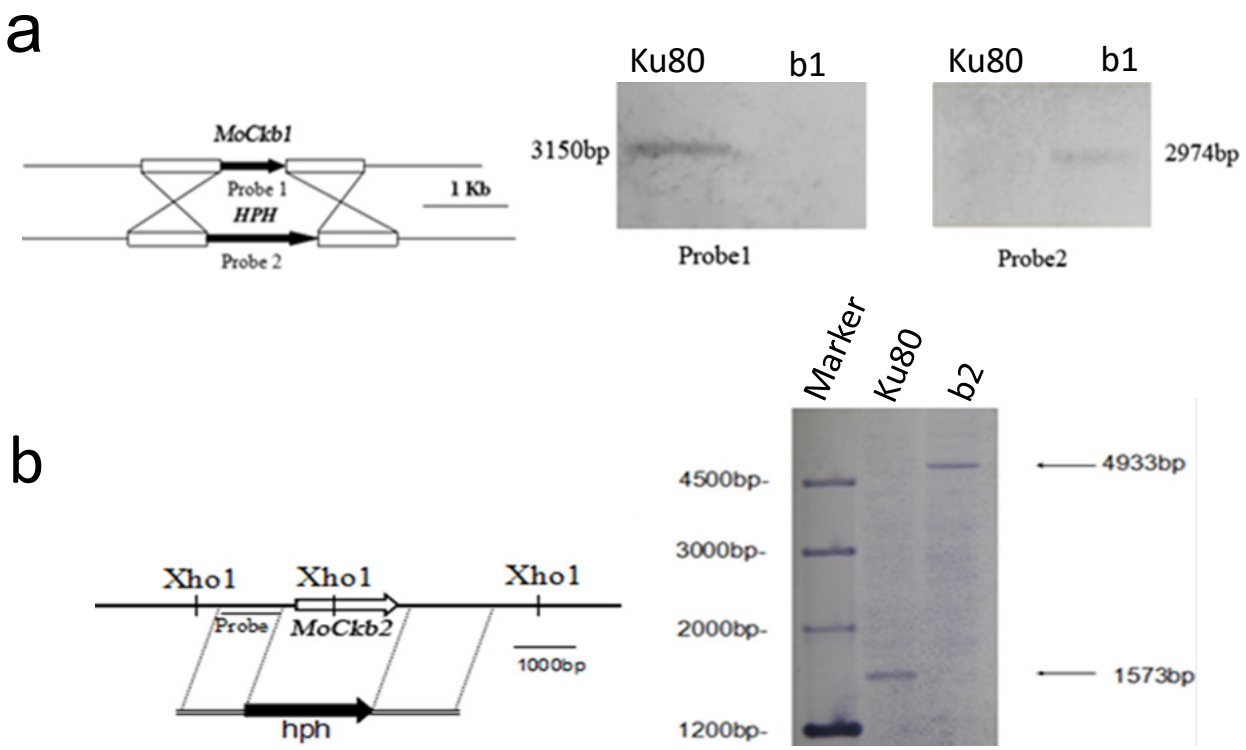

Figure 1. Knockout of the MoCKbs and the effect of this on conidia morphology and MoCKa gene expression (**a**) *ΔMoCkb1* mutant (strain b1) was verified by Southern blot analysis. The genomic DNA extracted from the strains Ku80 and b1 was digested with *Nde1* and tested by Southern blot. The different probes ORF and hph were amplified from the genomic DNA of the wild type Ku80 and the plasmid pCX62 respectively.
(**b**) *ΔMoCkb2* mutant (strain b2) was verified by Southern blot analysis. The genomic DNA extracted from the strains *Ku80* and b2 was digested with *Xho1* and tested by Southern blot. The probe was amplified from the genomic DNA of the background strain Ku80.

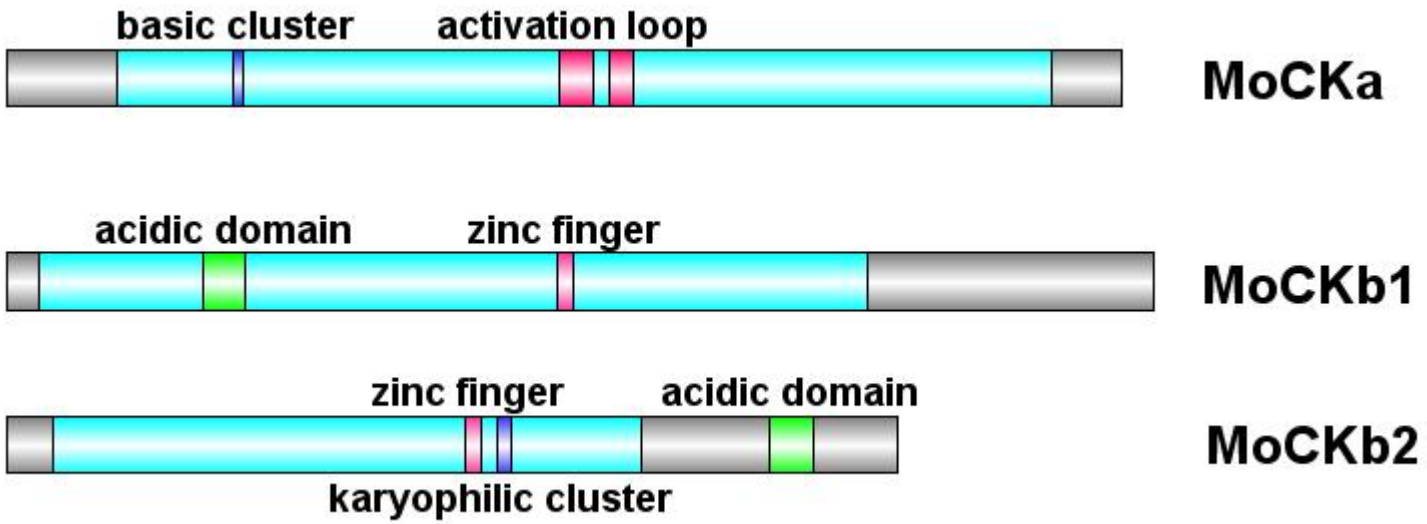

Figure 1 Supplement 1. Domain structure of the identified CK2 proteins.
MoCKa sequence (341 aa) was obtained from NCBI and the 35-320 region contains the protein kinase domain (https://www.ncbi.nlm.nih.gov/nuccore/XM_003716137.1) is labelled light blue, 70-73 is the basic cluster labelled dark blue and functions as a nuclear localization signal (NLS), 170-180 and 185-192 are activation loops (A-loop) labelled red.
MoCKb1 sequence (351 aa) was obtained from NCBI and the 11-264 region contains the Casein kinase II regulatory domain (https://www.ncbi.nlm.nih.gov/protein/XP_003718622.1) labelled light blue, 61-74 is the acidic domain labelled green, 169-174 is the zinc finger domain labelled pink.
MoCKb2 sequence (273 aa) was obtained from NCBI and the 15-195 region is the Casein kinase II regulatory subunit domain (https://www.ncbi.nlm.nih.gov/protein/XP_003710544.1) labelled light blue, 141-146 is a zinc finger labelled pink, 151-155 is a karyophilic cluster labelled dark blue that functions as a NLS, 234-247 is an acidic domain labelled green. The illustration was made using the DOG 2.0 Visualization of Protein Domain Structures http://dog.biocuckoo.org/.

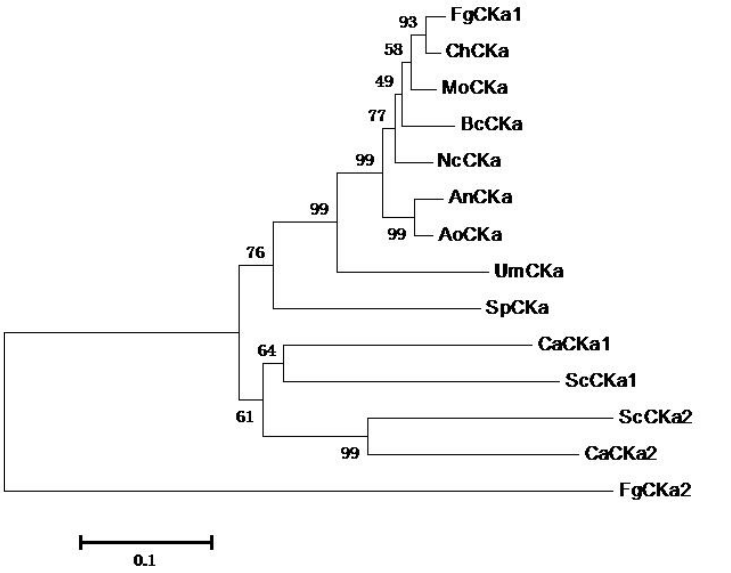

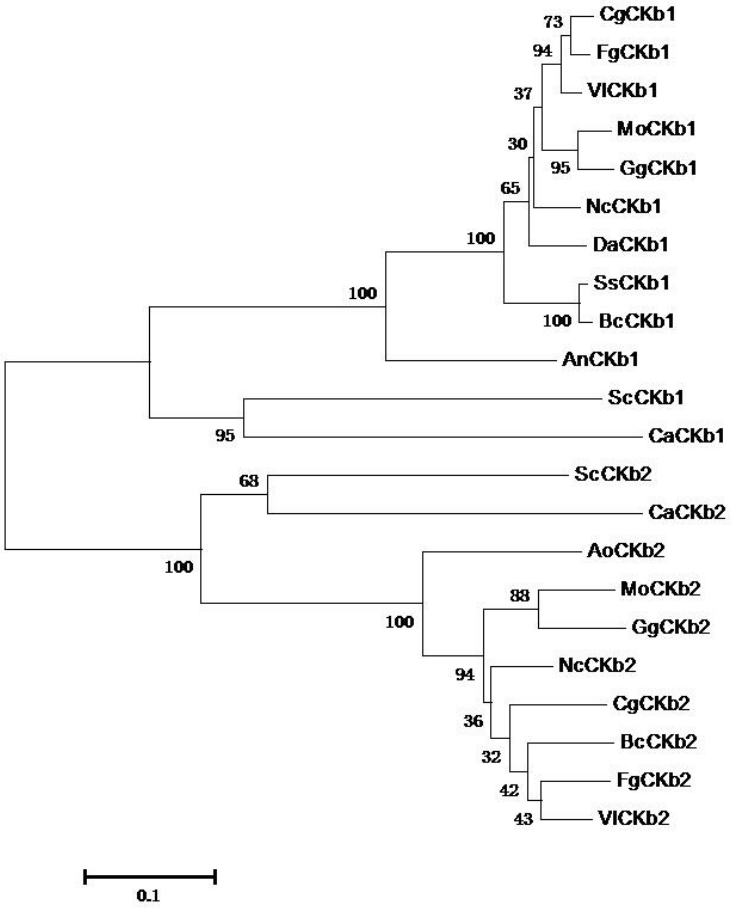

Figure 1 Supplement 2 (**a**) Phylogenetic analysis of CKa amino acid sequences from a range of organisms. A neighbor-joining tree was constructed from amino acid sequences of a range of CKa-encoding genes from diverse fungi. Tree topology was tested by 1000 bootstrap resampling of the data. Full species names and access codes for the annotated genes are given in Figure 1 Supplement 2 legend. **(b)** Phylogenetic analysis of CKb amino acid sequences from a range of organisms. A neighbor-joining tree was constructed from amino acid sequences of a range of CKb-encoding genes from diverse fungi. Tree topology was tested by 1000 bootstrap resampling of the data. Full species names and access codes for the annotated genes are given in Figure 1 Supplement 3 and Figure 1 Supplement 4 legends.

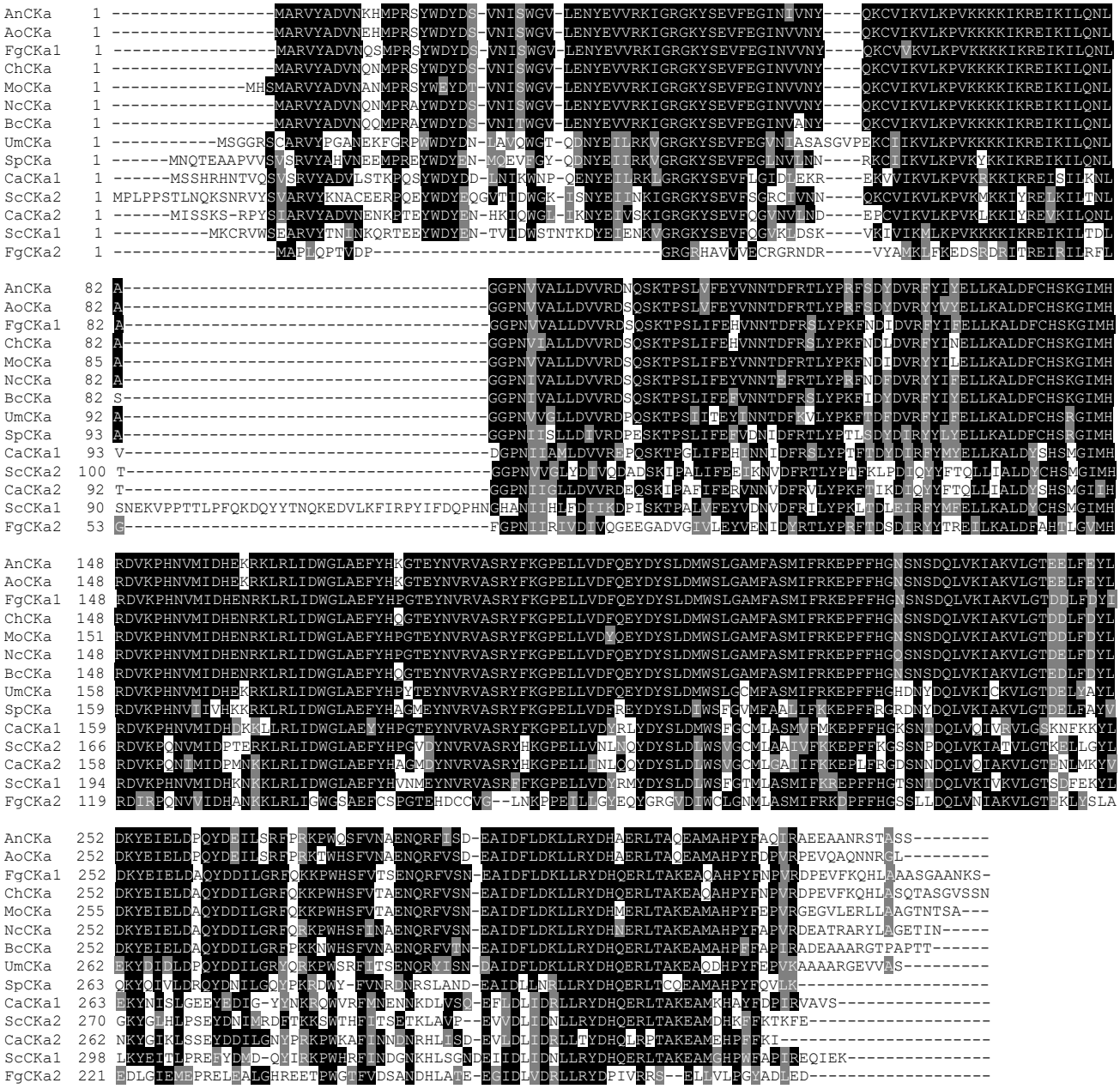

Figure 1 Supplement 3. Alignment of predicted amino acid sequences of CKa from different fungi. Sequence for the CKa in *M. oryzae* and other fungi were aligned using ClustalW and shaded by Boxshade 3.2. Identical amino acids are highlighted on a black background and similar amino acids on a light grey background. The *M. oryzae* amino acid sequence is aligned with the sequences of the putative homologs:

AnCKa (*Aspergillus nidulans*, EAA64615.1),
AoCKa (*Aspergillus oryzae*, KDE76853.1),
FgCKa1 (*Fusarium graminearum*, EYB33507.1),
FgCKa2 (*F. graminearum*, EYB32538.1),
ChCKa (*Colletotrichum higginsianum*, CCF36406.1),
MoCKa (*M. oryzae,* EHA49866.1),
NcCKa (*N. crassa*, EAA35747.3),
BcCKa (*Botrytis cinerea*, EMR85876.1),
UmCKa (*Ustilago maydis*, XP_011387122.1),
SSpCKa (*Schizosaccharomyces pombe*, CAA52331.1),
CaCKa1 (*Candida albicans*, KGU14189.1),
CaCKa2 (*C. albicans*, KGU00855.1),
ScCKa1 (*S. cerevisiae*, EDN61459.1),
ScCKa2 (*S. cerevisiae*, EDN63928.1).

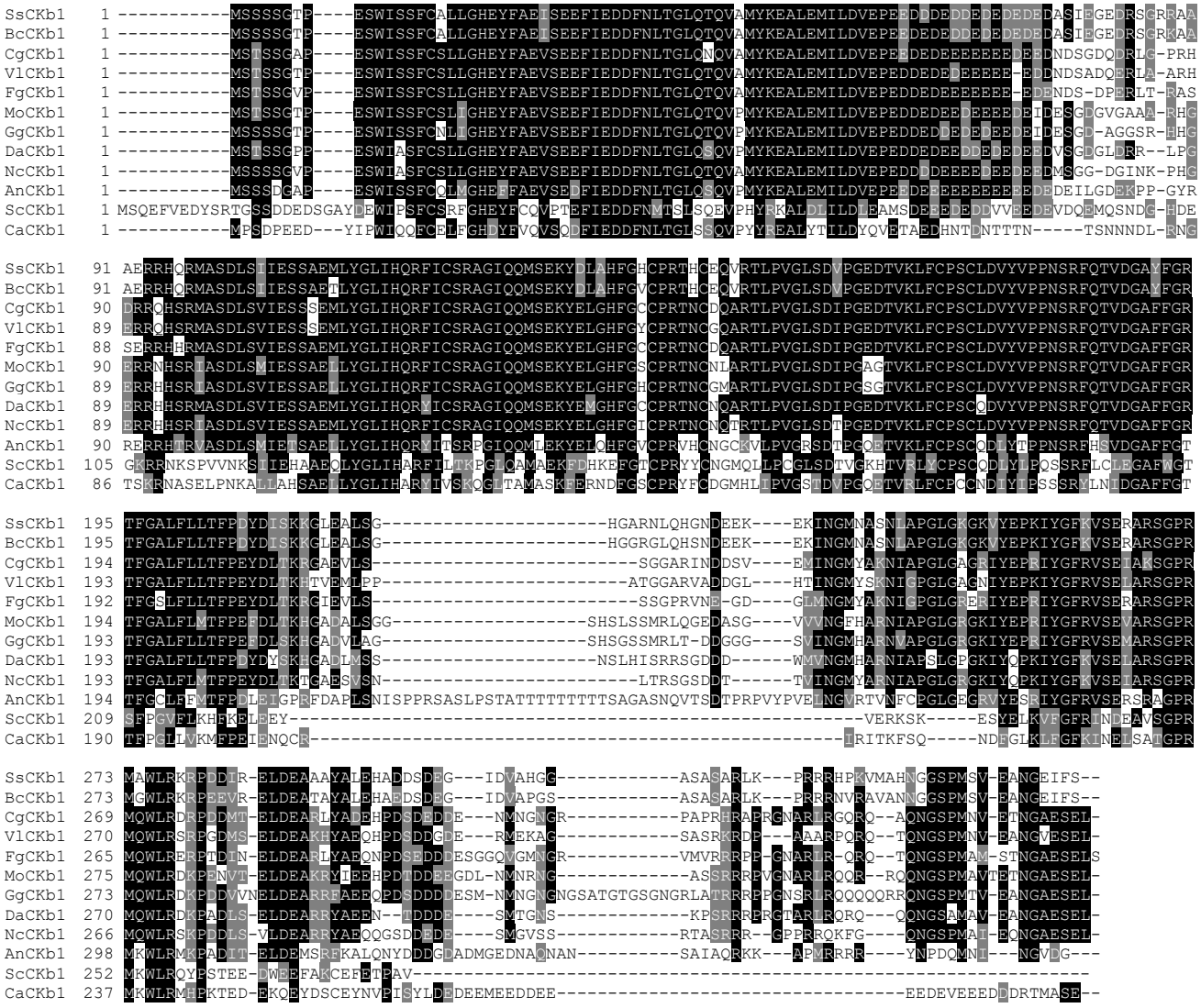

Figure 1 Supplement 4. Alignment of predicted amino acid sequences of CKb1 from different fungi. Sequence for the CKb1 in *M. oryzae* and other fungi were aligned using ClustalW and shaded by Boxshade 3.2. Identical amino acids are highlighted on a black background and similar amino acids on a light grey background. The *M. oryzae* amino acid sequence is aligned with the sequences of the putative homologs:

MoCKb1 (*M. oryzae*, XP_003718622.1),
GgCKb1 (*Gaeumannomyces graminis*, XP_009229023.1)
CgCKb1 (*Colletotrichum graminicola*, XP_008099475.1),
NcCKb1 (*N. crassa*, XP_960447.1),
FgCKb1 (*F. graminearum*, XP_011320142.1),
SsCKb1 (*Sclerotinia sclerotiorum*, XP_001592667.1),
BcCKb1 (*B. cinerea*, XP_001546938.1),
DaCKb1 (*Diaporthe ampelina*, KKY35702.1),
VlCKb1 (*Verticillium longisporum*, CRK29524.1),
AnCKb1 (*A. nidulans*, CBF77758.1),
ScCKb1 (*S. cerevisiae,* NP_011496.3),
CaCKb1 (*C. albicans*, KHC46950.1).

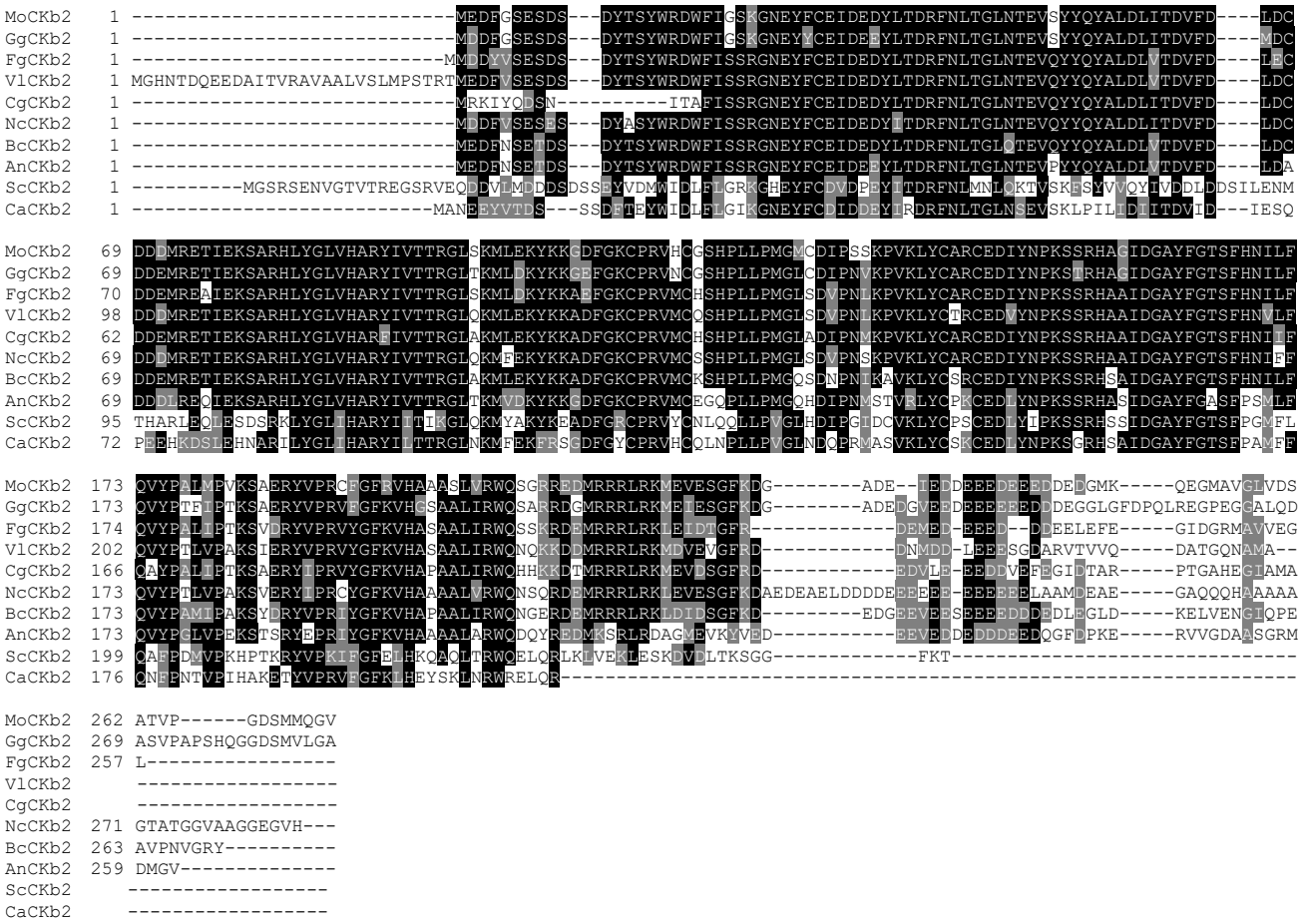

Figure 1 Supplement 5. Alignment of predicted amino acid sequences of CKb2 from different fungi. Sequence for the CKb2 in *M. oryzae* and other fungi were aligned using ClustalW and shaded by Boxshade 3.2. Identical amino acids are highlighted on a black background and similar amino acids on a light grey background. The *M. oryzae* amino acid sequence is aligned with the sequences of the putative homologs:

MoCKb2 (*M. oryzae*, XP_003710544.1),
GgCKb2 (*G. graminis*, XP_009217338.1),
FgCKb2 (*F. graminearum*, EYB21652.1),
VlCKb2 (*V. longisporum*, CRK18911.1),
CgCKb2 (*C. graminicola*, XP_008092732.1),
NcCKb2 (*N. crassa*, XP_001728406.1),
BcCKb2 (*B. cinerea*, XP_001558441.1),
AnCKb2 (*A. nidulans*, XP_001825358.2),
ScCKb2 (*S. cerevisiae*, AAT93000.1),
CaCKb2 (*C. albicans*, EEQ46313.1).

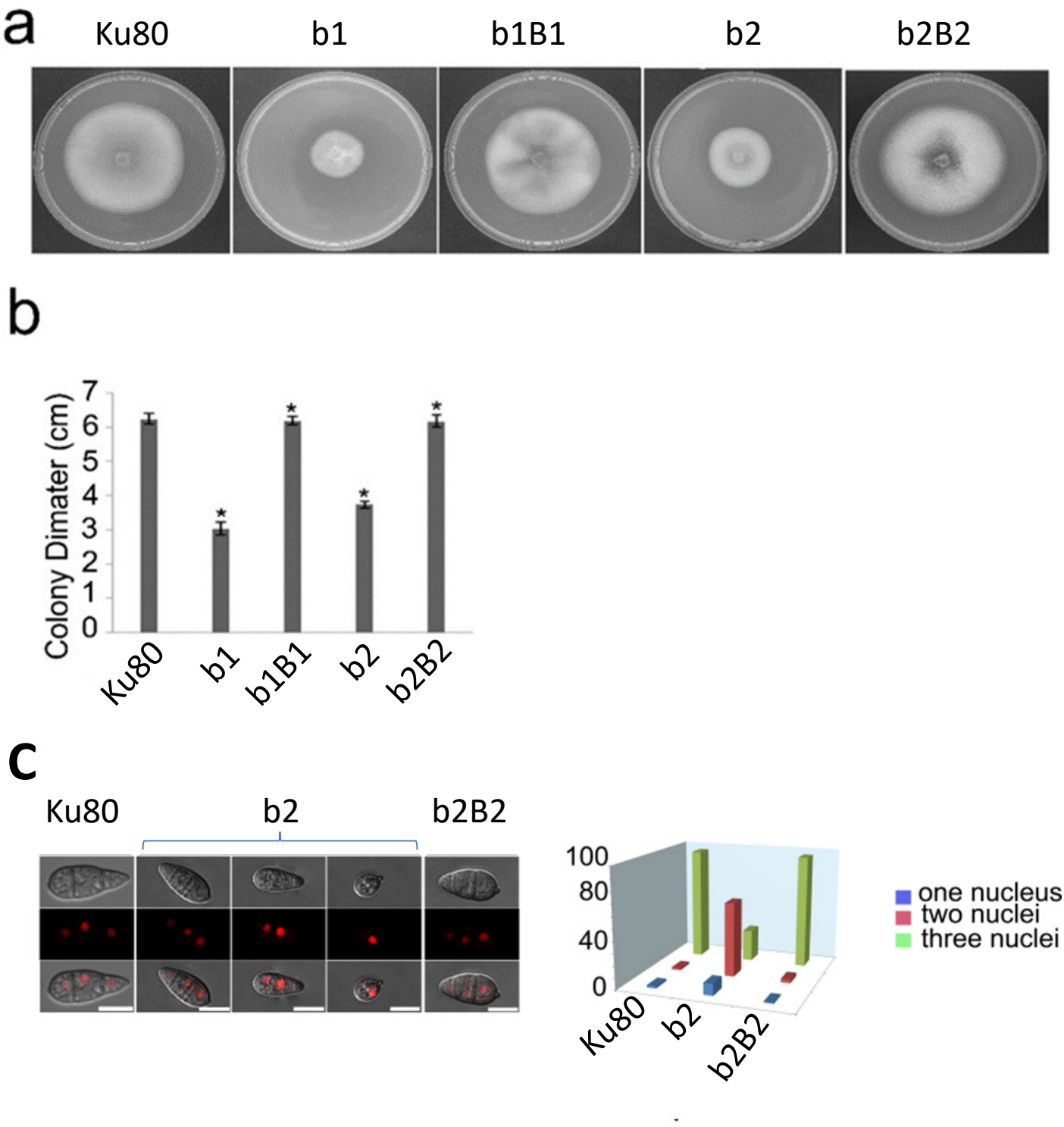

Figure 2. Intact CK2 holoenzyme is needed for normal growth, infection, pathogenicity. a, Colonial morphology and **b,** vegetative growth of *ΔMockb1* and *ΔMockb2* deletion mutants (b1 and b2) and their respective complementation strains (b1B1 and b2B2) was observed on SYM agar plates incubated in the dark for 10 days at 25°C, and then photographed. **C (left)** The conidial morphology of the *ΔMockb2* deletion (b2) was detected and compared to background (Ku80) and the complement (b2B2). The red fluorescence show the nuclear number in the conidia. The red fluorescence was due to the nuclear protein histone linker (MGG_12797) fused with mCherry used as nuclear marker. All bars = 10 um. **C (right**) The percentage of conidia with different nuclear number in the conidia produced by Ku80, b2 and b2B2. Error bars shows SE and a star indicate a P<0.05 for control is same or larger than for the mutants.

Figure 3. Control that strains GfpA, GfpB1 and GfpB2 are as pathogenic as the background Ku80. C is untreated control.

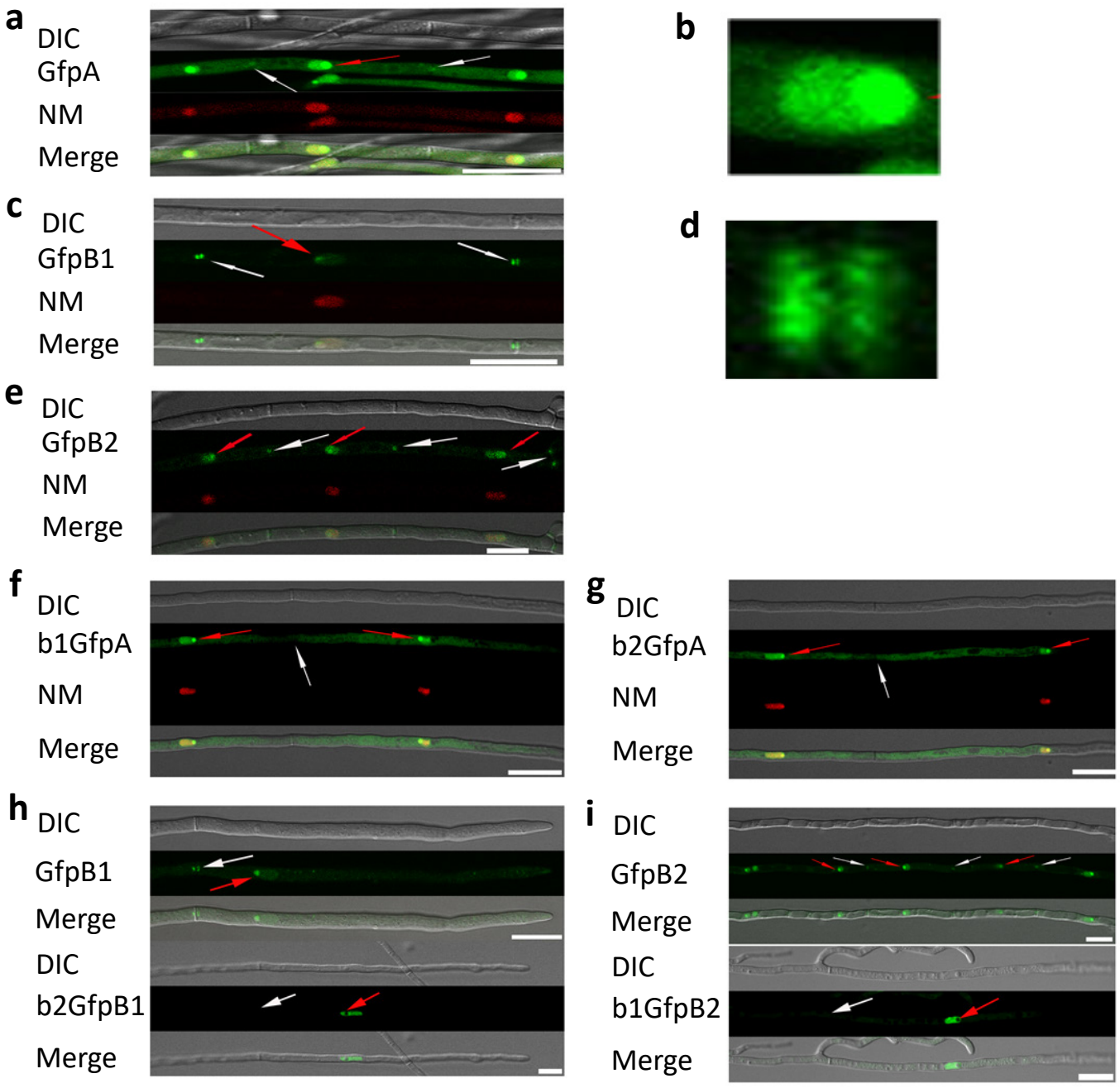

Figure 4. Intracellular localization of the three CK2 holoenzyme components showing that all three proteins are needed for normal localization. a-e, Localization of the three MoCK2 subunits in the background strain Ku80. The background strain Ku80 was transformed through gene replacements using plasmids containing GFP-MoCKa, GFP-MoCKb1 and GFP-MoCKb2 (Strains GfpA, GfpB1 and GfpB2). All three GFP constructs localize preferentially to nucleoli and to septal pores between cells. **b**, Enlargement of the nuclear localization of GFP-MoCKa (marked with red arrow in **a**). **d**, Enlargement of the septal localization of GFP-MoCKb1 (left septa marked with white arrow in **c**) **f** and **g**, Localization of over expressed GFP-MoCKa in *ΔMockb1* (b1GfpA) or in *ΔMockb2* (b2GfpA) does not rescue normal localization to septal pores. **h** and **i**, (below) Neither overexpression of MoCKb1 in *ΔMockb2* (b2GfpB1) nor overexpression of MoCKb2 in *ΔMockb1* (b1GfpB2) rescued normal localization (GfpB1 and GfpB2) (above) to nucleoli or septal pores. Histone linker (MGG_12797) was fused with the mCherry and used as nuclear localization marker (NM). All bars=10um.

Figure 4 Supplement 1.
GFP-MoCKa localization in conidia of strain GfpA.

Magnaporthe oryzae conidia.

GFP-MoCKa localizes to nuclei (red arrows) and to septal pores (white arrows). White bar is 10 μm.

a

Expression of	Control	Test	Test/control	SE (N=9)	P=same or higher than control
MoCKa	Ku80	b1	0.38	0.01	2.07E-11
MoCKa	Ku80	b2	0.54	0.05	5.12E-06

b

Expression of	Control	Test	Test/control	SE (N=9)	P=same or lower than control
MoCKa	b1	b1GfpA	25.11	1.32	4.23E-08
MoCKa	b2	b2GfpA	14.60	1.45	6.85E-06

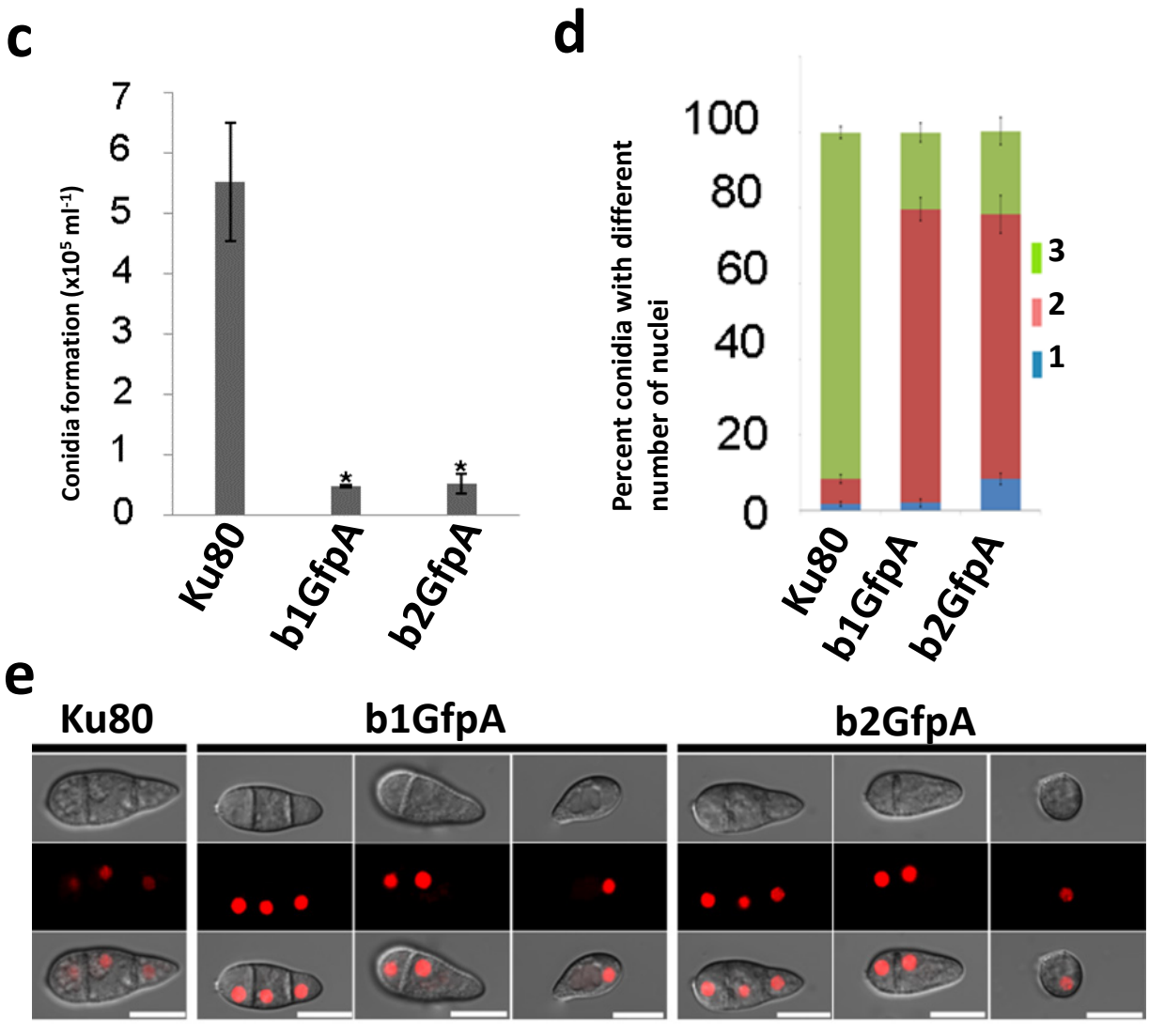

Figure 5. Overexpression of MoCKa in the MoCKb deletion mutants and the effect of this on conidia morphology. (**a**) MoCKa expression in the *ΔMockb1* and *ΔMockb2* deletion strains (b1 and b2) relative to the control Ku80 showing that expression of the other CKb were both reduced in the CKb deletion mutant (**b**) The relative expression of MoCKa in the b1GfpA and b2GfpA in relation to their respective control backgrounds b1 and b2. (**c**) The conidial forming ability of the transformant strains b1GfpA and b2GfpA compared to the background strain Ku80. (**d**) The percentage of conidia with different numbers of nuclei produced by the background strain Ku80 and the b1GfpA and b2GfpA strains and (**e**) the conidia morphology of the three strains. The red fluorescence was due to the nuclear protein histone linker (MGG_12797) fused with the mCherry used as nuclear marker. All bars = 10 um.

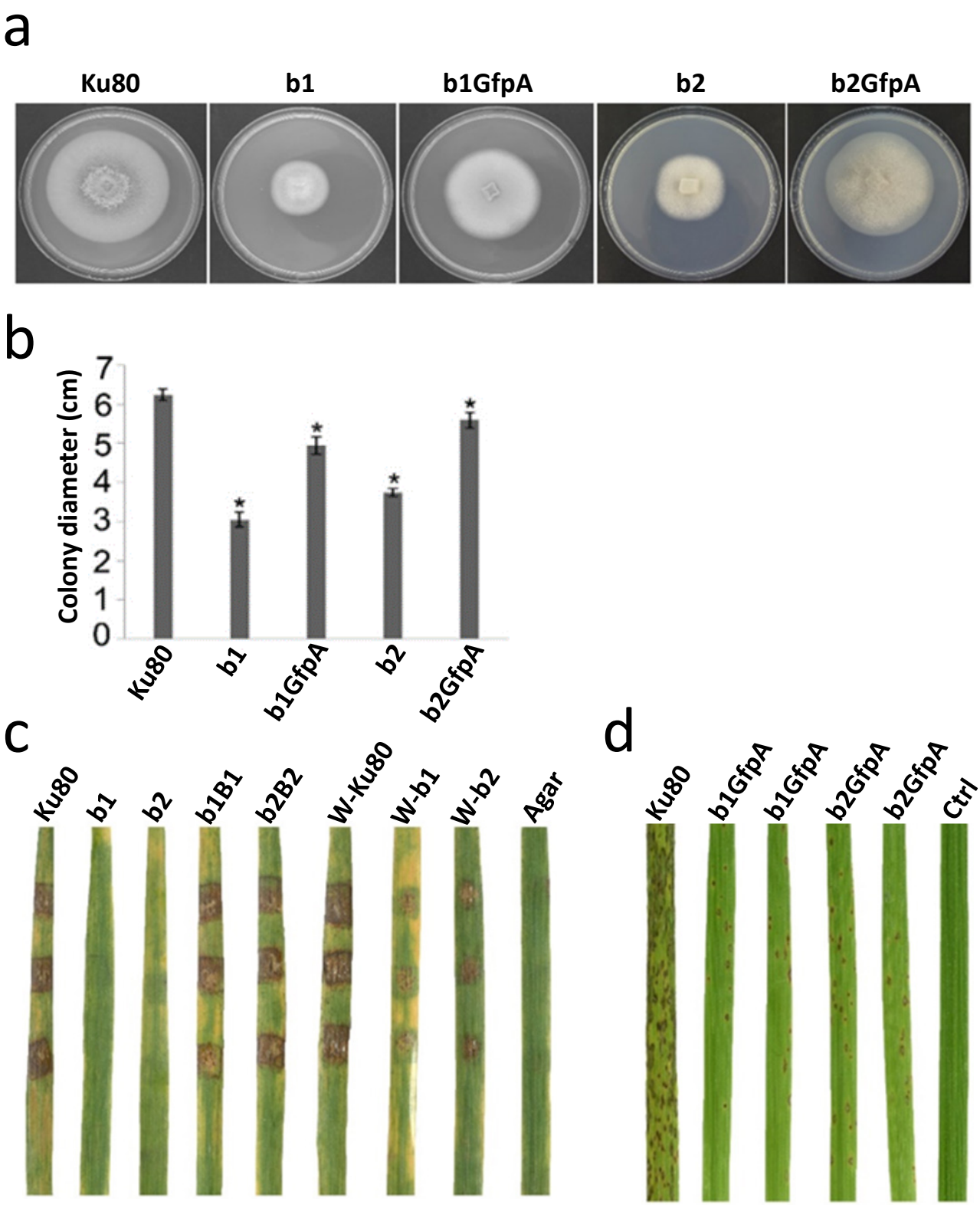

Figure 6. Intact CK2 holoenzyme is needed for normal growth, infection, pathogenicity. a, Colonial morphology and **b,** vegetative growth of *ΔMockb1*, *ΔMockb2*, (Strain b1 and b2) and overexpressed GFP-CKa in b1 (b1GfpA) and in b2 (b2GfpA). Strains were grown on SYM medium agar plates incubated in the dark for 10 days at 25°C, and then photographed. **c,** Pathogenicity analysis strains b1 and b2 on rice. Disease symptoms on rice leaves of 2-week-old seedlings inoculated using mycelial plugs since mutants produced no or very few conidia. Typical leaves were photographed 6 days after inoculation. The b1B1and b2B2 were complementary strains. Treatments starting with a W indicate that the leaf surface was wounded before mycelial plug was applied. The rice cultivar was CO-39. **d,** Pathogenicity analysis of overexpressed GFP-CKa in strain b1 (b1GfpA) and b2 (b2GfpA). Disease symptoms on rice leaves of 2-week-old seedlings inoculated with conidia suspension since CKa overexpressed strains produced just enough conidia to use for the assay. The concentration of conidia in the suspension was about 1×10^5/ml. Typical leaves were photographed 6 days after inoculation. The rice cultivar was CO-39. Error bars shows SE and a star indicate a $P<0.05$ for that the control is same or larger than for the mutants.

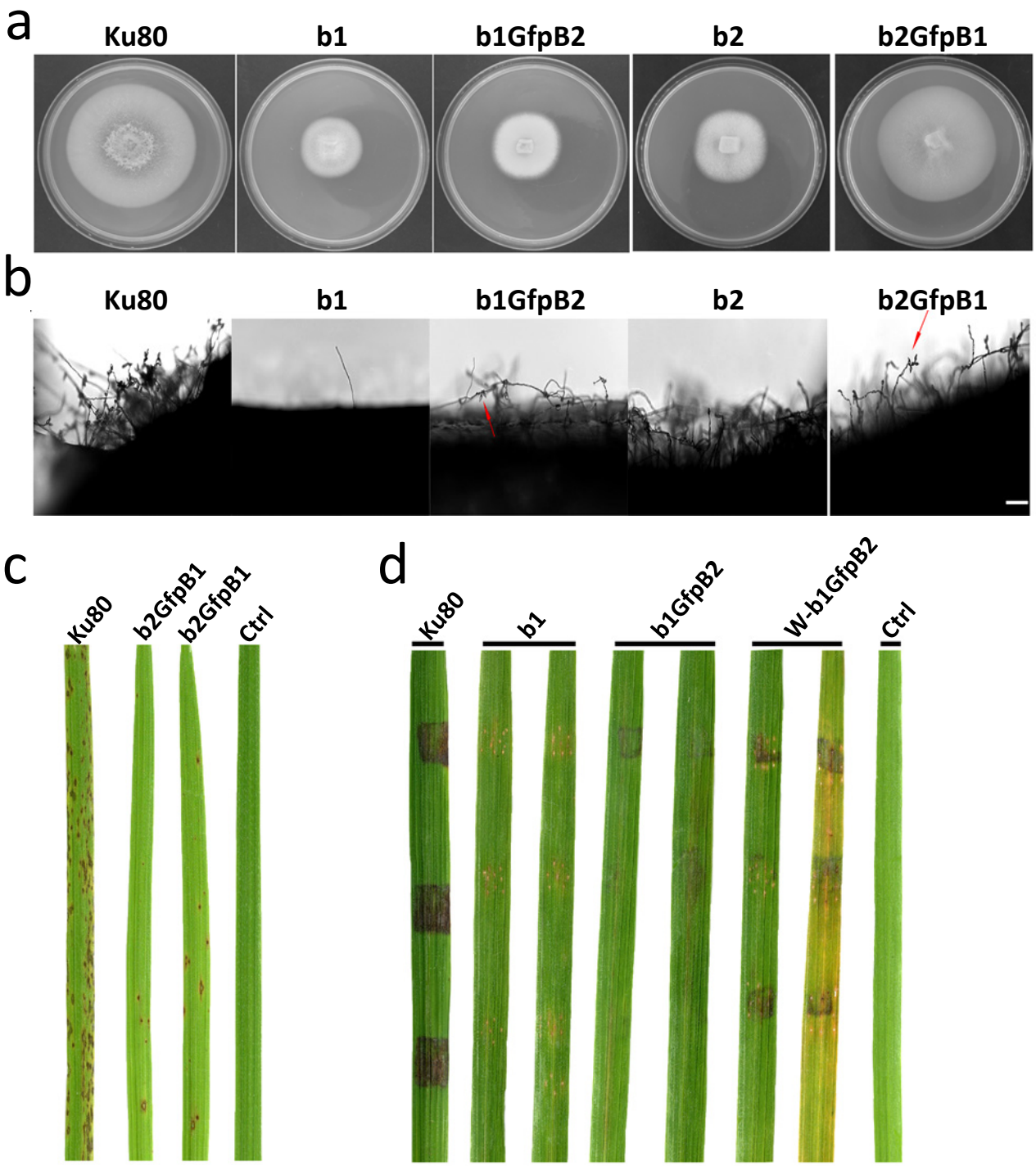

Figure 6 Supplement 1. Phenotypic effects in the respective MoCKb deletion mutants of overexpression the other MoCKb component. (**a**) Colonial morphology and vegetative growth of strain b1, b1GfpB2, b2 and b2GfpB1 transformants was observed on SYM medium agar plates grown in the dark for 10 days at 25 °C and then photographed.

(**b**) Development of conidia on conidiophores. Light microscopic observation was performed on strains grown on the rice bran medium for 10 days. The red arrows indicate some conidia are produced by the b1GfpB2 and b2GfpB1 strains. Bar=50um.

(**c**) Pathogenic analysis of the b2GfpB1 strain. Disease symptoms on rice leaves of 2-week-old seedlings were also inoculated by conidia suspension. The concentration of conidia suspension for inoculation was about $1x10^5$/ml.

(**d**) Pathogenic analysis of b1 and b1GfpB2 strains on rice. Disease symptoms on rice leaves of 3-week-old seedlings were inoculated using mycelial plugs. The W-b1GfpB2 indicates that the rice leaves were wounded before the agar plugs were placed. Typical leaves were photographed 6 days after inoculation. The rice strain was CO-39.

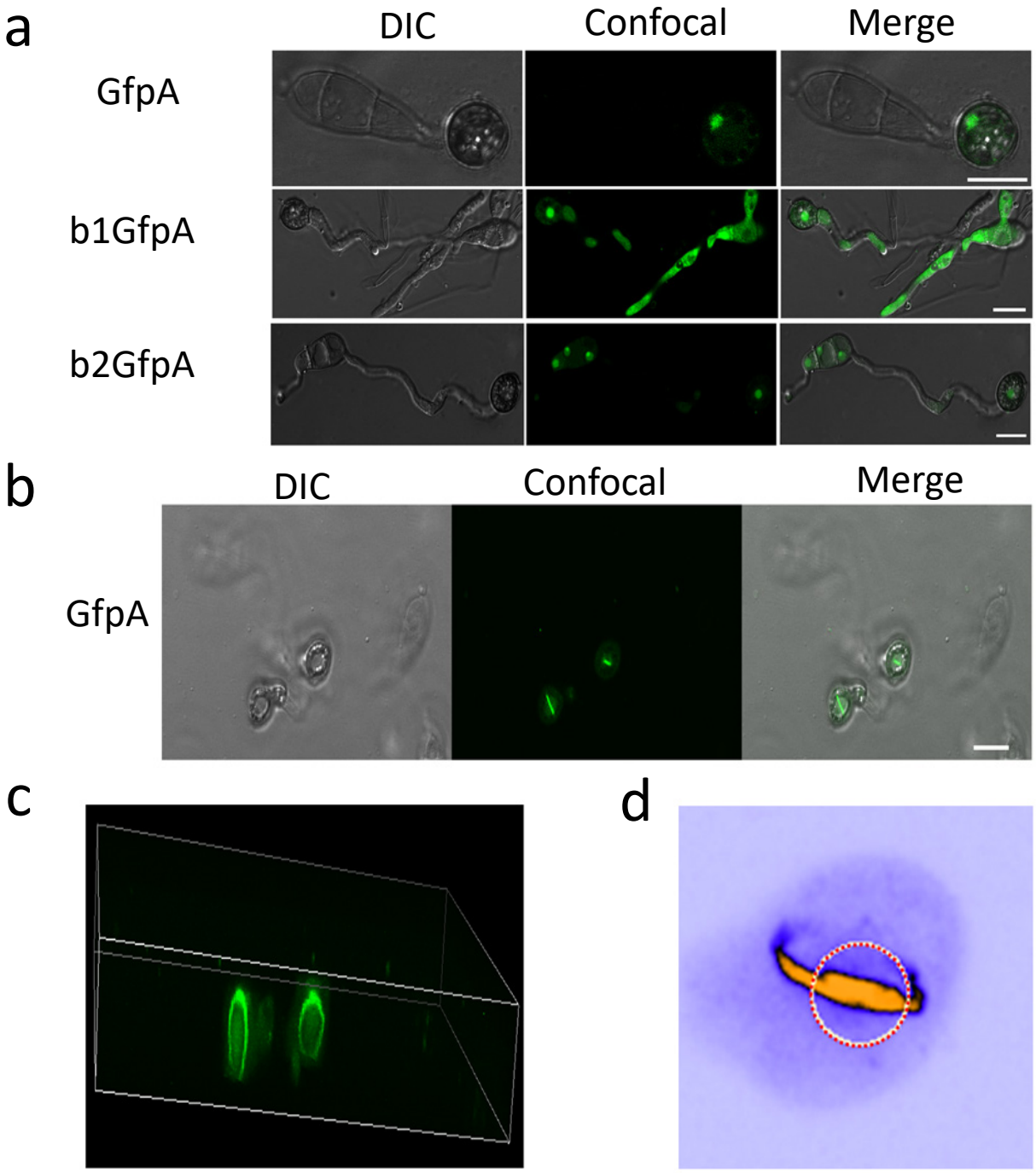

Figure 7. Localization of the GFP-MoCKa subunit in appressoria of the background strain Ku80 (strain GfpA) the and in the two MoCKb deletion strains (b1GfpA and b2GfpA) (compare Fig. 1a, f, g). **a,** Localization of GFP-MoCKa in all three strains show localization to nuclei**. b,** In the strain GfpA that form appressoria from conidia a bright line of GFP-MoCKa can be seen across the appressorium penetration pores. **c.** Through 3d scanning and then rotating the 3d reconstruction image (Link to Movie 1) we found that the streak across the penetration pores is a ring of GFP-MoCKa perpendicular to the penetration pore opening not present in the deletion strains b1GfpA and b2GfpA (Link to Movie 2 and 3). **d,** False colour lookup table 3d reconstruction image of the right ring structure in **c** enlarged and rotated back and seen from the same angle as in **b** with the penetration pore opening indicated by a red-white circle seen from the "plant" side (Link to Movie 4 and 5 for left and right ring in false colours). The false colour was used so that the week fluorescence in the cytoplasm could be used to show the whole cytoplasm volume. The image was made using the analytical image analysis freeware ImageJ (https://imagej.nih.gov/ij/index.html) and the ICA lookup table in ImageJ was used for false colouring.**.** All bars=10 μm.

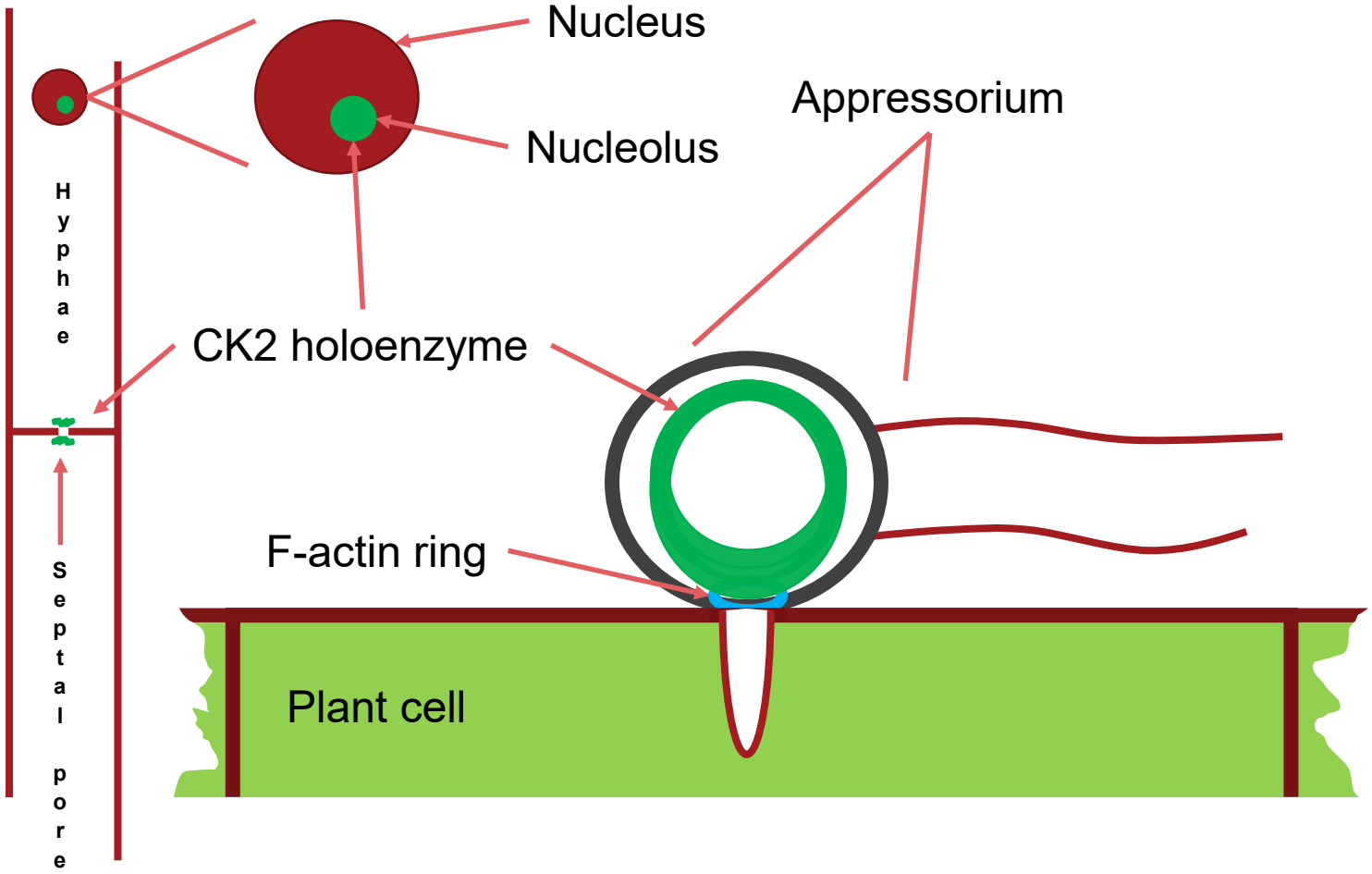

Figure 8. Schematic drawing of the main localizations of the CK2 holoenzyme. It localizes to the nucleolus, to septal pores between cells and forms a large ring structure perpendicular to the F-actin ring surrounding the appressorium penetration pore. Appressorium and hyphae drawn approximately to their relative sizes.

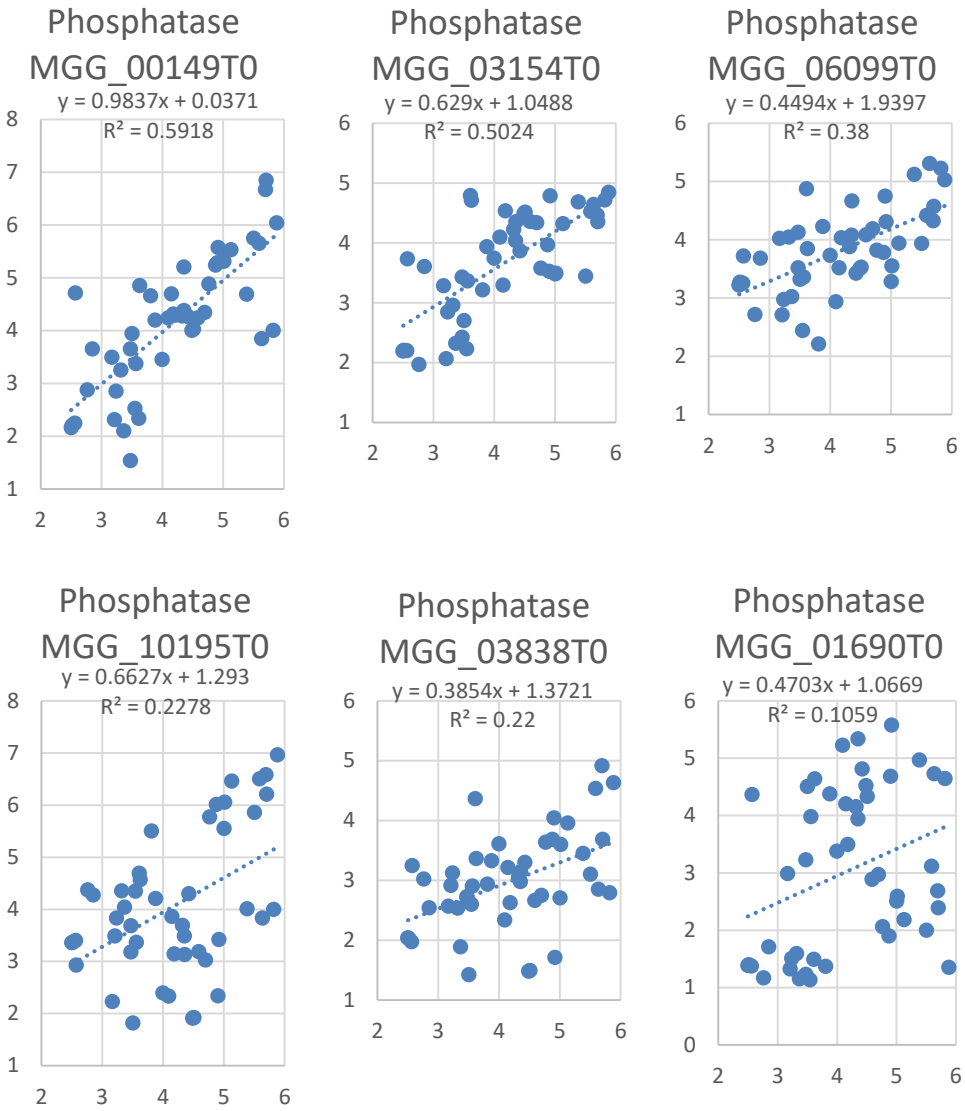

Figure 9. Plots of 6 putative serine/threonine protein phosphatase expression (y-axis) vs MoCKa expression (x-axis) in a range of transcriptome datasets from different experiments (Note: Log2 scale on axes and grids are represented with fixed "aspect ratio" to highlight the different slopes of the correlations). MGG_01690 is not in the pulldown while the other five are and used to illustrate that not all S/T phosphatases are well correlated with CKa. The P values for the Null hypothesis of no correlation with CKa are: MGG_00149 P=2.7E-10, MGG_03154 P=2.5E-8, MGG_06099 P=4.0E-6, MGG_10195 P=6.9E-4, MGG_03838 P=8.8E-4, MGG_01690 P=2.6E-2
Transcriptomic data was downloaded from public websites so as to be able to test the relationship under many different growth conditions in many experiments.

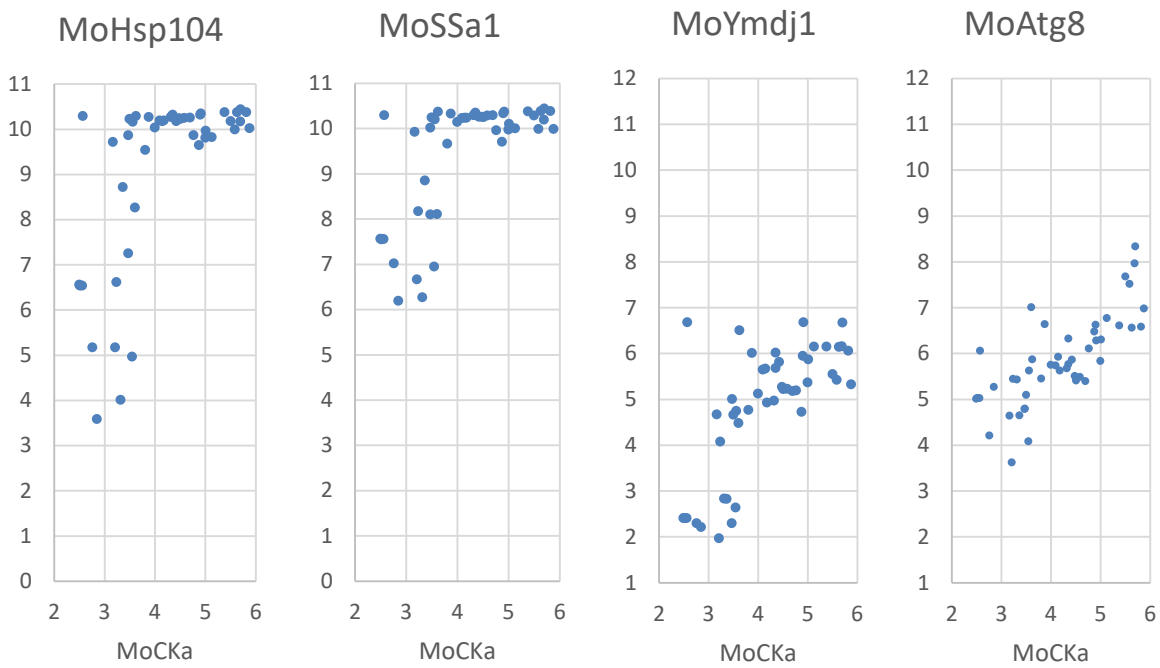

Figure 10 Plot of expression involved in protein quality control vs MoCKa expression in a range of transcriptomes from different experiments (Note: Log2 scale on axes and grids are represented with fixed "aspect ratio" to highlight the slope of the correlation). P value for the Null hypothesis that there is no correlation = 9.9E-10. Transcriptomic data was downloaded from public websites so as to be able to test the relationship under many different growth conditions in many experiments.
Hsp104, SSa1 and Ymdj1 has in yeast been shown to cooperatively help aggregate proteins to be able to refold. The key protein with its main function in this process appear to be Hsp104 (Glover and Lindquist, 1998).

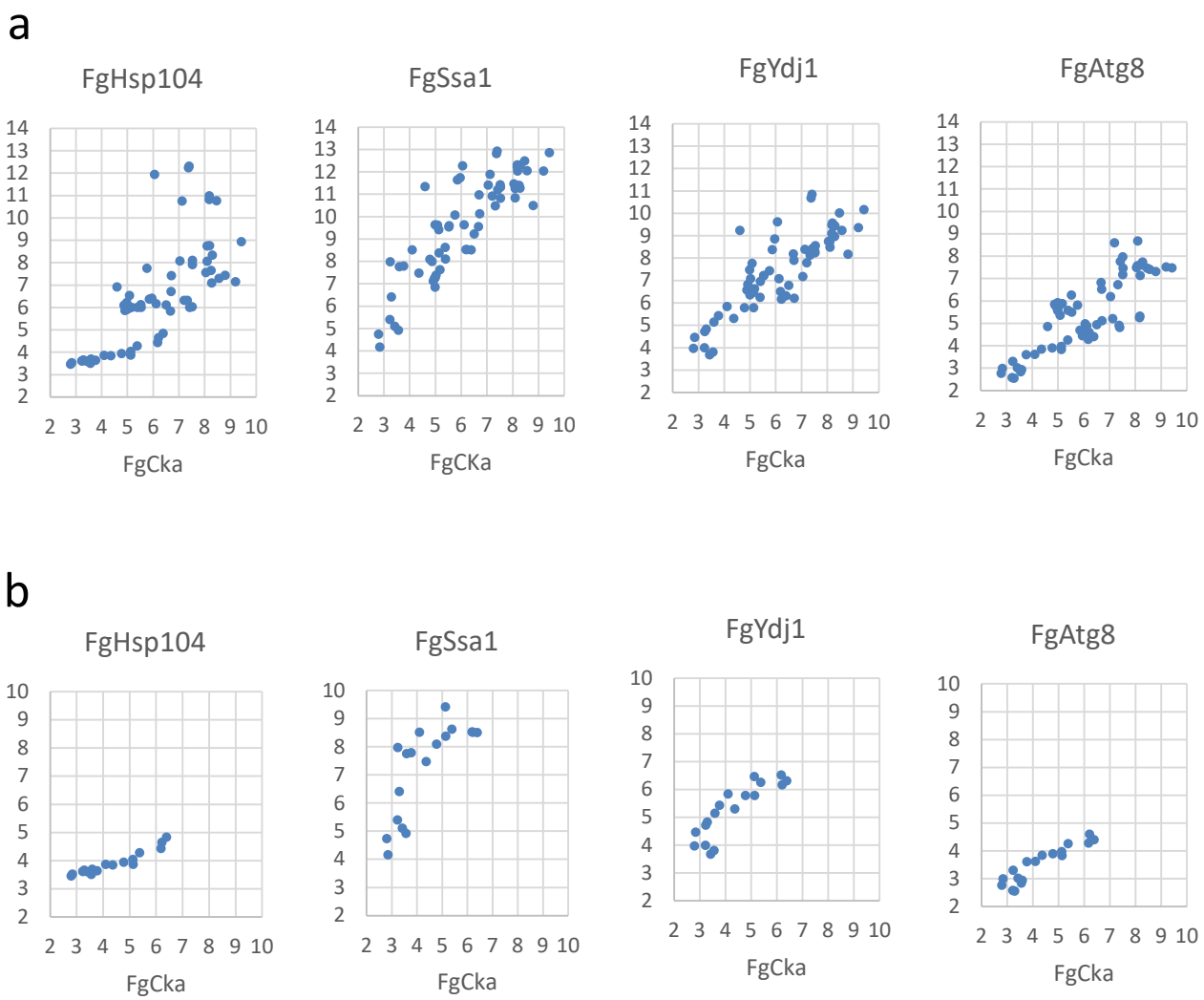

Figure 10 Supplement 1. Plot of expression involved in protein quality control vs FgCKa expression in a range of transcriptomes from different experiments (Note: Log2 scale on axes and grids are represented with fixed "aspect ratio" to highlight the slope of the correlation). a. data from all experiments. b data from a time course infection experiment (see Fig 10 supplement 2 for details on the time course of expression)

Transcriptomic data was downloaded from public websites so as to be able to test the relationship under many different growth conditions in many experiments.

Hsp104, SSa1 and Ymdj1 has in yeast been shown to cooperatively help aggregate proteins to be able to refold. The key protein with its main function in this process appear to be Hsp104 (Glover and Lindquist, 1998) .

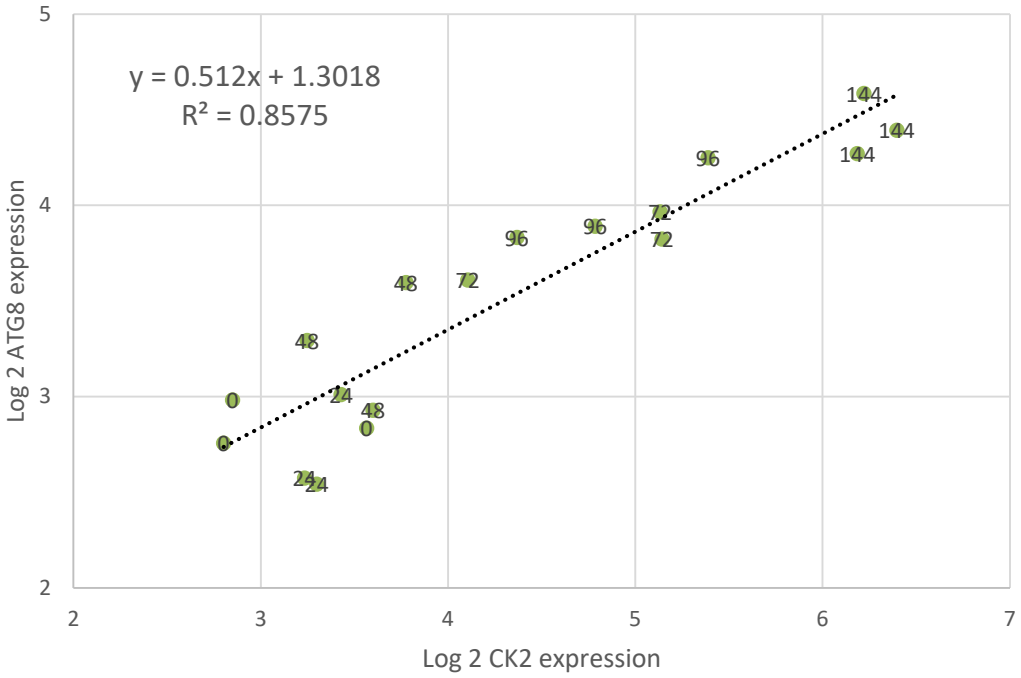

Figure 10 Supplement 2. Plot of FgAtg8 (autophagy) expression vs FgCKa expression in a times series infection experiment with 3 replicates where numbers in the plot indicate hours post infection (hpi). (Note: Log2 scale on axes and grids are represented with fixed "aspect ratio" to highlight the slope of the correlation). P value for the Null hypothesis that there is no correlation = 3.6E-08 . Transcriptomic data was downloaded from public websites so as to be able to test the relationship under many different growth conditions in many experiments.

Table 1 Background and mutant strains of *M. oryzae* used in this study

Strains	Genotype description	Reference
Ku80	*ku80* deletion mutant of Guy11 (Background strain in this study) containing CKa (A), CKb1 (B1) and CKb2 (B2), thus contains AB1B2 alleles. The other strains are labelled according to the changes introduced.	35
b1	*Mockb1* deletion mutant of *Ku80*	This study
b2	*Mockb2* deletion mutant of *Ku80*	This study
b1B1	*ΔMockb1* transformed with the wild-type MoCKb1 protein	This study
b2B2	*ΔMockb2* transformed with the wild-type MoCKb2 protein	This study
b1GfpA	*ΔMockb1* transformed with the over-expressed GFP-MoCKa fusion protein	This study
b2GfpA	*ΔMockb2* transformed with the over-expressed GFP-MoCKa fusion protein	This study
b1GfpB2	*ΔMockb1* transformed with the over-expressed GFP-MoCKb2 fusion protein	This study
b2GfpB1	*ΔMockb2* transformed with the over-expressed GFP-MoCKb1 fusion protein	This study
GfpA	Ku80 transformed with the over-expressed GFP-MoCKa fusion protein	This study
GfpB1	Ku80 transformed with the over-expressed GFP-MoCKb1 fusion protein	This study
GfpB2	Ku80 transformed with the over-expressed GFP-MoCKb2 fusion protein	This study

Table 2 Primers used in this study

Primer name	The sequence of primer（5’→ 3’）
3696qRTF	CGTCAACTACCAGAAATGCG
3696qRTR	TGACGGAGTCTTGCTCTGTG
446qRTF	GCAGAGGTGTCGGAGGAAT
446qRTR	CCAAGATCATCTCCAGTGCC
5651qRTF	ACCCGTTGCTGCCGATGG
5651qRTR	TAGACCTGGAAGAGGATGTTGTGG
Tub1RTF	CAACATCCAGACCGCTCTC
Tub1RTR	ACCGACACGCTTGAACAG
446AF	GCCCAACCTTTCATCCTA
446AR	TTGACCTCCACTAGCTCCAGCCAAGCCTACCTCCAGTGCCTCCTT
446BF	GAATAGAGTAGATGCCGACCGCGGGTTCTCGTCCAACTCTAAACTAAC
446BR	GCTGGGTAAACATCTCATT
5651AF	GGGGTACCCCCTCTAAGTGGTCGTGC
5651AR	CCGGAATTCCTTGGATGGAATTGTGCC
5651BF	CGCGGATCCAGGGAGGCGTTATCATTTA
5651BR	TAATCTAGACAGAGCCGAGCTTGTCTA
446comF	GCTCTAGAGCGGAACCAGTAGTTGACGG
446comR	GGGGTACCCATGACAACGCCGGAGGG
5651comF	GCTCTAGAGCCCGACAAGCACAAAAGAT
5651comR	CCCCCGGGGAGCGTTCGTTTAGACCC
3696GFPF	CGGGATCCATGCACAGCATGGCACGC
3696GFPR	CGGAATTCTGTTGAAATTACCAGCGATTC
5651GFPF	CGGGATCCATGGAAGATTTTGGCAGCG
5651GFPR	CCCTCGAGTCAGACACCTTGCATCATG